POLITECNICO DI TORINO

Master's Degree in Physics of Complex Systems

Master's Degree Thesis

Optimal Channel Networks

Supervisors

Prof. Luca RIDOLFI

Prof. Amilcare PORPORATO

Candidate

Luca GIACCONE

December 2023

Abstract

Channel networks are ubiquitous in our world. They are found in biological systems as intricate blood capillary structures, in natural landscapes as river drainage patterns, and even in various human transport designs such as urban water supply networks. This thesis embarks on a comprehensive exploration of over a century of Optimal Channel Networks (OCNs) literature. Our aim is to formulate a unified model that captures and generalizes the cumulative efforts done in this field. We have provided a complete mathematical description of the optimization process, arguing that the commonly assumed 'principle of local optimality' is, probably, dispensable. Our generalization not only synthesizes the existing knowledge about optimal networks but also try to introduce fresh perspectives, including a new explanation for the formation of loops even in a stationary regime, a modern picture of the optimal network landscape and the revelation of a phase transition within the ground state topology of these networks. This findings enhances our understanding of the intricate interplay between channel networks structure and optimization, shedding light on previously unexplored facets of this fascinating field.

Table of Contents

Chapter 1

Introduction

The problem of efficiently distributing (or draining) resources among numerous receivers (donors) represents a challenge that must be addressed frequently in our world. This happens in nature, where living organisms have to develop in a way to constantly supply every cell with fundamental vital substances. River drainage networks, with their interesting geometries, are an other example of natural solution to this problem. Moreover, the same issue is faced in engineering, for instance, in the design of effective electrical distribution implants or water supply/drainage networks. In general, if the elements that require (furnish) the supplies are very close to the source (collector), diffusion is the best transport mechanism that can guarantee an efficient transfer of resources. Conversely, often we deal with situations where the size of the system is not so small to make diffusion efficient. Channel networks arise to overcome this inefficiency of diffusion for large-scale transport (Fig. 1.1). In particular, in this thesis, we studied Optimal Channel Networks (OCNs). We call them '*Optimal*' since, in principle, there are many ways to realize those linkage structures, but not all possible designs are equally convenient. We expect, for instance, that nature, during eras of evolution, has managed to design very specific and efficient channel arrangements. Therefore, on the other hand, when we address technological problems, we would like to be able to plan intelligent solutions. The theoretical research on OCNs has always been deeply influenced by natural evidence, and one major goal in this field still is to try to capture the evolutionary wisdom we previously discussed. Besides that, our progress in the comprehension of this problem seems to point out that, usually, nature follows a good constructional design, but maybe not the best one. This is due to the complex path that every natural system has to pass through during its development. Therefore, in the end, in this field are very important both the 'best designs', that we hope to be able to employ for technological applications, and either the statistics of the just 'good designs', that can be reached through imperfect search in the complex space of networks arrangements.

Our discussion starts by giving a historical perspective in Chapter 2. Beginning with the early 1900s, we are going to explore the major contributions and key ideas that we found in literature. The first steps in this field were directed towards understanding the local optimal properties of OCNs, famously giving rise to the Hess-Murray law. Only in a second moment, the global network features assumed great interest. In particular, the differences coming from stationary or time-dependent transport regimes are quite relevant. Notably, it is in the time-dependent regime where optimal solutions exhibit the emergence of non-trivial loops. Furthermore, this chapter ends with the brief exploration of an alternative methodology, the so-called adaptive approach.

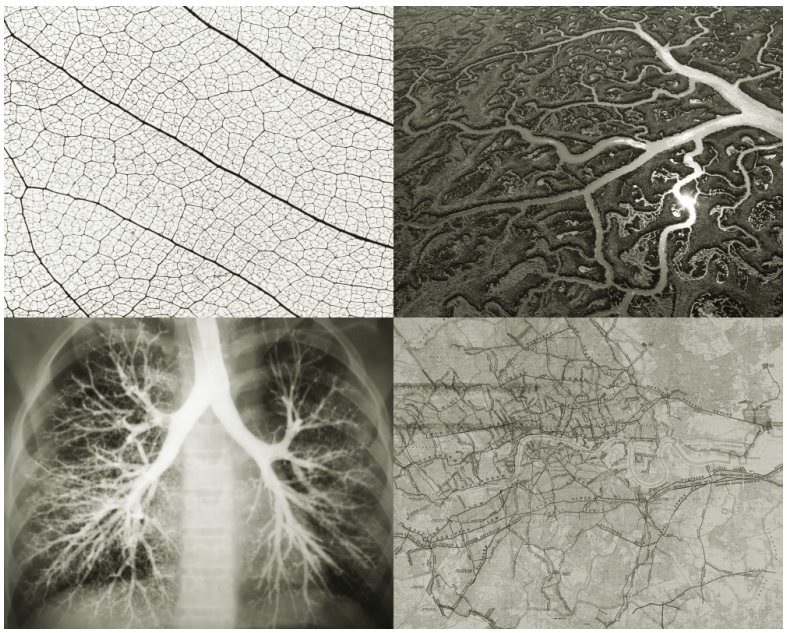

Figure 1.1: Examples of channel networks: close view of leaf venations (upper left corner), above view of the Guadalquivir river (upper right corner), X-ray of the human lungs (lower left corner) and the map of London sewers (lower right corner).

In Chapter 3, the discussion of our true research begins. We are going to propose the description of a unified model for OCNs. Here, we first give the mathematical characterization of our proposal, and then we try to present a systematic picture of the optimization framework. This chapter also explores the dichotomy existing between constrained or unconstrained models. Notably, we challenge the conventional belief in the 'principle of local optimization,' arguing its real necessity. In the end, we discuss some new behaviors that seem to arise from our model.

Chapter 4 addresses the technical description of the algorithms toolkit we employed to generate optimal networks. All the presented algorithms have been coded in Python during the time devoted to this thesis, and they served as a means to evaluate numerically our model. We present various strategies, outlining their advantages and defects.

A crucial point of our discussion is the definition of a cost function to evaluate different network performances. Chapter 5 is dedicated to an investigation into the current state of knowledge concerning the minima landscape of the mentioned cost function. The latter is defined in a very high-dimensional space, and furthermore, it can be shown that the number of its minima grows exponentially with the dimension of the domain. We try to resume the findings gathered in the literature in a unique phase diagram while introducing novel details. Most notably, we show the existence of a phase transition within the topologies of networks at their ground state.

In the concluding chapter, we synthesize our results and present together the threads that we hope to deepen in future research. This thesis tries to offer a comprehensive view of optimal channel networks, passing through historical antecedents, contemporary optimization methodologies, and numerical analyses towards a modern picture of OCNs.

Chapter 2

Optimal channel networks

In nature, it is frequent to see intricate network structures designed for the efficient transport of resources. These networks are exemplified by the human circulatory system, the lymphatic networks found in plants, or the complex channel systems associated with river drainage basins. The great elegance and functionality of these interconnected systems have moved scientific curiosity and started an inquiry for practical applications. In this chapter we will provide a concise overview of the pivotal ideas that have contributed to our understanding and modeling of optimal channel networks, tracing the evolution of knowledge from its inception to the contemporary state of research.

2.1 Local optimality and Hess-Murray law

The research history of optimal channel networks has its roots in the work of two pioneering physiologists, Walter Rudolf Hess and Cecil Dunmore Murray. They both worked in the early 900' trying to understand the local (about each channel separately) characteristics that make natural network efficient. Hess, a Swiss physiologist and Nobel prize winner, first proposed the principles of what would later become known as the Hess-Murray Law. In his 1914 doctoral thesis Hess introduced the concept of a "work minimization" principle governing the circulation of blood or lymph within living organisms. Using this idea he was able to determine the vessel radius that would incur the least energy expenditure for an organism. Just as an historical remark, we can mention that in his 1808 Croonian Lecture [1], Thomas Young, proposed the same result found by Hess [2] without providing any theoretical justification. Later on, Cecil D. Murray, an American physiologist, "rediscovered" the Hess-Murray Law in 1926 [3], further expanding its significance. Murray's analysis was primarily focused on identifying the most efficient means of oxygen transport within the human body. Murray echoed Hess's ideas by starting

with the assumption that the power required in a single vessel, of length l and radius r, can be written as:

$$J = \Delta P Q + bV = c_1 \frac{Q^2}{r^4} + blr^2 \tag{2.1}$$

where ΔP is the pressure gradient in the pipe, Q is the volumetric flow, b is a constant and V is the volume of the vessel. Note that the second equality is obtained in hypothesis of laminar flow. Thus Murray took into account two contribution to the power. The first is straightforwardly the energy needed to sustain the flow in the vessel. The second is the metabolic cost of building and maintaining the conduit. From (2.1) it is then a simple mathematical problem to obtain that it exists an optimal value for the vessel radius:

$$\begin{aligned} r^* &= \left(\frac{2c_1}{bl}\right)^{\frac{1}{6}} Q^{\frac{1}{3}} \\ r^* &\propto Q^{\epsilon} \qquad \epsilon = \frac{1}{3} \end{aligned} \tag{2.2}$$

it should be stressed that, this first fundamental result on the optimal structure of networks, is therefore completely 'local'. In the sense that it is only related to any individual channel but it is not telling us anything about the global structure of the net. Despite that, we can even see another interesting consequence of (2.2) by considering continuity at bifurcations (Fig.2.1):

$$\begin{aligned} Q_0 &= Q_1 + Q_2 \\ r_0^3 &= r_1^3 + r_2^3 \end{aligned} \tag{2.3}$$

the latter is precisely the relation commonly referred to as Hess-Murray law. In the following years this law has been widely discussed [4]. Uylings [5] showed that (2.2) can be generalized to turbulent flows obtaining $\epsilon = 3/7$. An exponent $\epsilon = 1/2$ can be derived in pulsatile flow [6]. Miguel [7] showed that the optimal radius depends on the "degree of non-Newtonianity" of the fluid, ω, and than (2.2) can be more generally rewritten using an exponent $\epsilon = 2/(3\omega + 3)$ (with $\omega = 1 \implies$ Newtonian fluid). Several experimental findings, as documented in references [8], [9], [10], [11], and [12], have been gathered. These studies took into consideration vascular and aerial networks in various animal species, as well as lymphatic networks in plants. The collective results of these experiments suggest that the exponent ϵ could exhibit a range between 1/3 and 1/2, with some studies even extending this variability further.

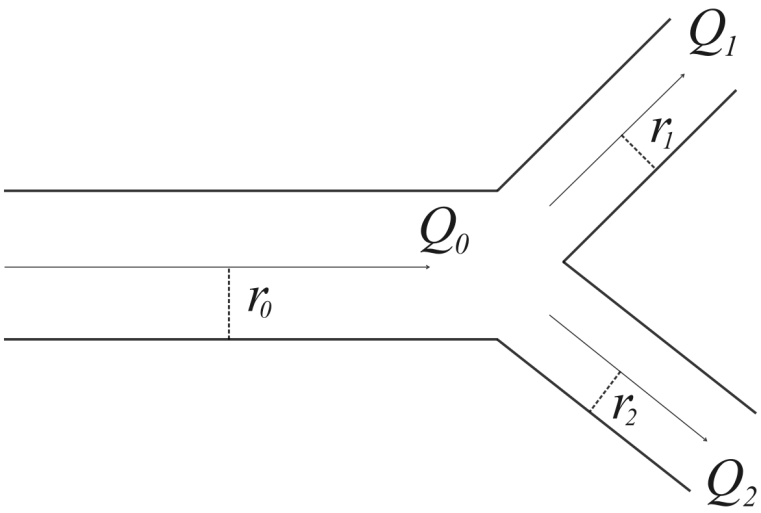

Figure 2.1: Network bifurcation

Notably, the predictions of the H-M Law were found to be more accurate for smaller vessels, such as arterioles and capillaries, underscoring its significance, as well as its limits, in understanding the design of circulatory and branching systems within living organisms. The Hess-Murray Law continues to be an important concept in the study of optimal transport networks, keeping track of the fundamental work of these two physiologists and their enduring impact on the field. In conclusion, in order to stress one last time the importance of this law, we can recall the words that Sherman used in a well-documented review [13] of the Hess-Murray Law:

> *Murray's law for connecting large vessels to small is as memorable as Pythagoras' edict on right triangles*
>
> Thomas F. Sherman [13]

2.2 The stationary problem

Subsequent years witnessed a shift in focus from local structures to the examination of global organizational principles within transport networks. Researchers began representing these networks as conductance graphs, introducing the concept of total energy cost, i.e. the cumulative energy per unit time required for the establishment and maintenance of the whole network. A conductance graph is a weighted graph where each link represent a pipe of the network and the relative weight stands for the conductance of that link. We will define more properly the conductance in chapter 3, but for the moment let's just think that a pipe with higher conductance allow for a larger flow, whereas as the conductance goes to zero the link can accommodate less and less flow. If a link is not present in the network its conductance is null. Additionally, at each node in the network, an exogenous flux is defined. This concept is significant for various applications. In biological systems, it can represent the idea that each node either demands or supplies a specific quantity of resources. In the context of river drainage networks, this exogenous flux may symbolize the input of rainfall. In human systems, these exogenous fluxes correspond to the demands of individual entities within the network. This conceptual framework provides a foundation for understanding the common characteristics of various types of transport networks, it provides the basis to try to understand how resources are distributed within these complex systems.

There is in particular one research group that was able to reach decisive breakthroughs and helped to develop a rich picture of OCNs, working continuously on this field for the last thirty years. The principal authors of this group are Rodríguez-Iturbe, Rinaldo, Banavar and Maritan. The first great step ahead was due to the establishment of some principles postulated behind the structure of optimal networks. Those principles were thought as intuitions arising from the experience gathered with experimental evidence on natural networks. In particular in the 90' Rinaldo and Rodríguez-Iturbe [14] [15] [16] [17] stated the existence of a 'principle of local optimality' and a 'principle of global optimality'. The first is essentially just equivalent to say that the network should fulfill the Hess-Murray optimality condition (2.2) at each edge. Note that this is far from obvious the edges being not independent. The second states that the network should minimize a global cost of the form:

$$J = \sum_e J_e \tag{2.4}$$

where the sum span all the edges and the term J_e is the cost of the *e-th* edge. The application of the 'local optimality' principle is fundamental since it simplifies dramatically the mathematical description of the system. In particular if we constrain our analysis only to network fulfilling (2.2) at each edge, it can be easily

shown that (2.4) can be written only in terms of the flows as:

$$J = \sum_e f_e(Q_e) \tag{2.5}$$

this is a central result that soon would have lead to deep consequences. In fact not much later, in 2000, Banavar rigorously proved [18] an analytical result which still remains the foundation for current research in this field. His demonstration showed that the optimal structure of a network, with a cost function in the form of (2.5), is dependent solely on the concavity of the functions $\{f_e\}$. Note that it is crucial, for Banavar's well-known proof to hold, that the global cost can be expressed solely as a function of the flows Q_e. This idea led to the following conclusion: there exist two distinct categories of Optimal Channel Networks, characterized by fundamentally different properties, corresponding to convex and concave cost functions, respectively. If all $\{f_e\}$ functions are convex, the unique minimum of the cost corresponds to a completely looped geometry. On the other hand, if the functions are concave, there is a high redundancy of local minima, with every spanning tree representing a local optimum. It should be further considered that, the authors of the mentioned research group, were originally interested mostly in river networks. This is the reason why, if we go in depth into their formulation, they make use of a very specific shape for the cost function (2.5) that can be derived in the context of river flows. Despite that, in the following years, researchers attempting to study the optimal networks problem, even in different scenarios and for different kind of flows, were influenced by the great results just discussed. Notably a study by Bohn and Magnasco published in 2007 [19] showed that, even by starting with the well known models aiming to describe biological networks, at the end, using the same principles just discussed, the problem falls into the issue of minimizing a function in the form (2.5). Typically (more on that in Chapter 3) it can be shown that under the previous assumptions the global cost can be written as:

$$J \propto \sum_e Q_e^\Gamma \tag{2.6}$$

meaning that functions $\{f_e\}$ are simple power laws, all featuring the same exponent Γ, that therefore is responsible for their concavity. So the exponent Γ assumed a great interest since it is the parameter that allows for completely different kind of behaviours. Following the exact results by Banavar, one can say that, for $\Gamma < 1$, a huge number of local minima emerges, yet all maintain a tree-like structure. Conversely, for $\Gamma > 1$, a singular OCN configuration, where all links are present, dominates the others. In this regime, it became more economical to construct numerous links with small conductance values.

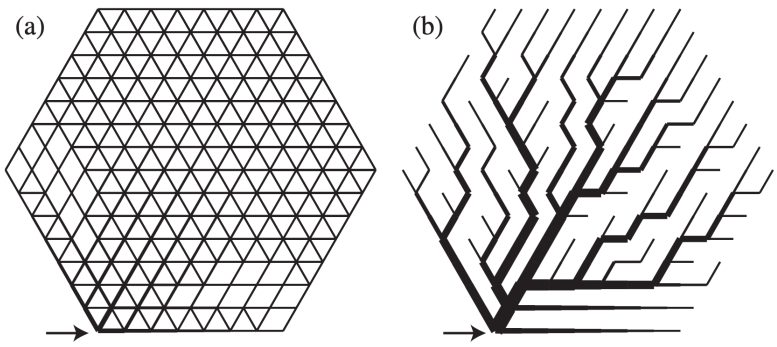

Figure 2.2: Results obtained by Bohn and Magnasco [19], in (a) we see the OTN for $\Gamma > 1$ while in (b) the $\Gamma < 1$ case is displayed

Let's conclude this section with a couple of remarks:

Remark 1. *Nowadays this result (phase transition between loopy and tree networks) is widely accepted and it is often taken as starting point for further analysis. On the other hand the initial set of arbitrary principles that lead to this conclusions has been no more questioned. It seems to us that the very roots of all the recent discussion about OCNs are often disregarded and just given as granted. But as we will show in next chapter we believe that it is now possible to go beyond the initial scheme of assumptions we presented in this section, towards a more general and lighter set of principles.*

Remark 2. *Beside its importance, this outcome underscores some intrinsic limitation of the described approach. In particular the hierarchical loop structures commonly observed in real-world natural networks can't be understood in this framework. The intricate complexities of these networks cannot be fully explained through the optimization of steady-state resource transport alone.*

2.3 Adding fluctuations and the appearance of loops

In recent times, the exploration of incorporating stochasticity and fluctuations into network models has gained significant interest. This development holds broad relevance because the classical assumption of stationary flow, commonly employed in the study of optimal networks, is an idealization that diverges from real-world complexities. In a work by Corson in 2010 [20], the concept of fluctuations was introduced by considering the vector of sources, representing resources injected at each point in the network, as a random variable.

In this stochastic framework, where the cost function is expressed in terms of average quantities, fluctuations gave rise to an entirely distinct category of optimal structures. These structures exhibited a blend of loops coexisting with the hierarchical organization of trees. Concurrently, in the same year, Katifori studied fluctuations through a distinct perspective [21]. First, he pursued a path analogous to Corson's approach, except that he introduced randomness by considering sinks, representing demands, as random variables rather than sources. Second, he explored the interesting concept of fluctuations as random damage to the network. Under this premise, any edge could potentially be eliminated with a certain probability and we can think to be optimizing the network also with respect to its robustness to stochastic malfunctioning or physical damage.

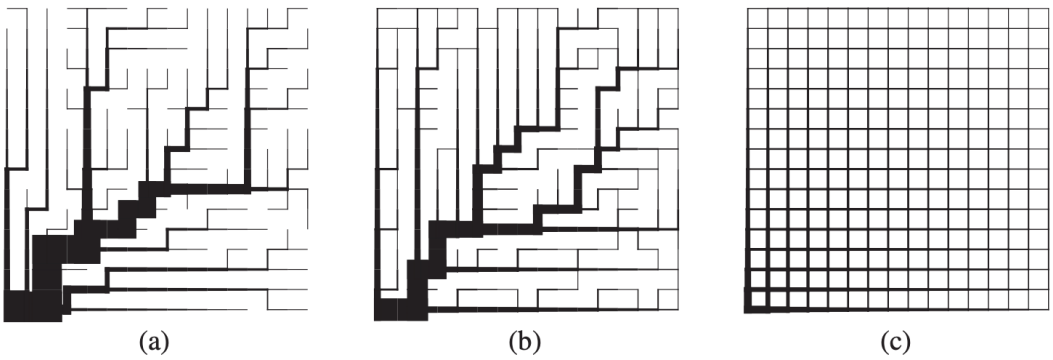

Figure 2.3: Results obtained by Corson [20], the same fluctuations strength characterize the three pictures whereas: in (a)$\Gamma = \frac{2}{5}$, (b) $\Gamma = \frac{6}{7}$, (c) $\Gamma = \frac{10}{9}$

Remarkably, in both of these distinct approaches, fluctuations leaded to a profound influence on the optimal structure of the network, favoring the presence of loops. Despite that, while hierarchical loops emerged in both models, the quantitative characteristics of the resulting networks exhibited clear disparities.

This exploration of fluctuations has expanded our understanding of optimal network topologies, underscoring the interplay between stochasticity and the formation of loopy structures.

Recently (2021-2023) Facca and Lonardi [22] [23] have shown that the appearance of loops is more generally the hallmark of non stationary flows. The same effect can be seen, as a particular case, by introducing stochasticity only because fluctuations lead to a non stationary regime.

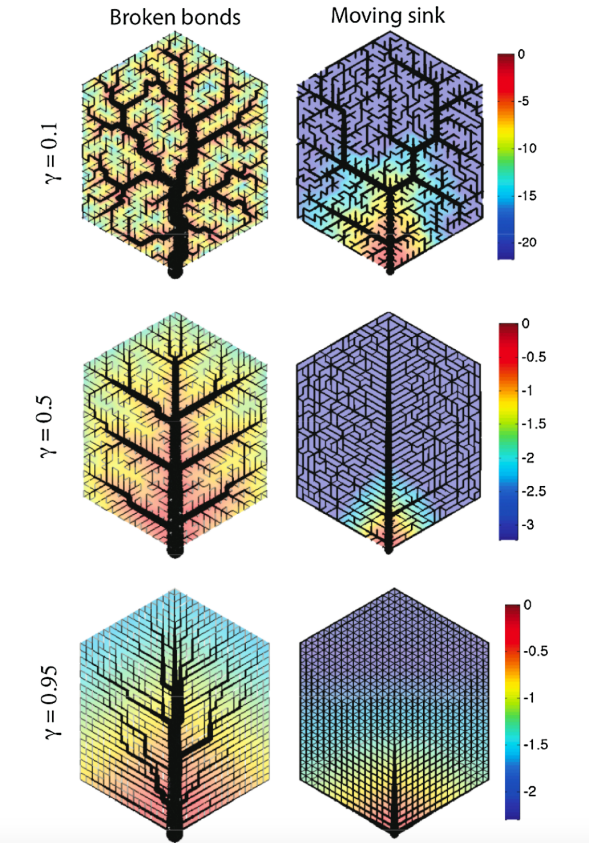

Figure 2.4: Results obtained by Katifori [21]. We can see the appearance of loops as a result of optimizing under damage to links (left column) and under a fluctuating load (right column). Note also that the colour scale marks the pressure gradient and γ does not exactly coincides with the previous discussed exponent Γ. But it can be shown that $\Gamma = \frac{2\gamma}{\gamma+1}$. In particular since $\gamma = 1 \iff \Gamma = 1$ they both denote a overall change of behaviour in a similar way.

2.4 The dynamical approach

It is important to stress that the conceptual pathway we are pursuing is not the sole approach that has been considered to address this problem. In a recent publication by Lu and Hu in 2022 [24] it is emphasized that historically, two distinct perspectives have guided investigations into this field.

The first approach, which is given by the trajectory we have explored in previous articles, is centered around the formulation of a cost function and an analytical optimization. Researchers operating within this paradigm imagine that nature, through an evolutionary process, has somehow managed to construct optimal network structures. Although the focus is not directly on the physical process that allow to realize an optimal network but just on the final outcome. The difficulty of this methodology lies in defining a proper cost function and subsequently solving an optimization problem to deduce the network's ideal configuration.

Conversely, the second approach [25] [26] [27] [28] [29] [30] directs its attention toward understanding the dynamic processes underlying network construction and optimization. The necessary starting point to proceed with this idea is to make an ansatz for the dynamical evolution of each pipe:

$$\frac{\partial C_i}{\partial t} = F(Q_i, C_i) \tag{2.7}$$

where C_i is the conductance of the *i-th* edge, Q_i is the flow passing thought the pipe and F is an ansatz function defining the dynamics. Usually the specific form of F is chosen giving some intuitive arguments and assumptions. The main recurrent ideas are that:

- the conductance should increase over time if a big flow pass into it (positive feedback)
- if the flow is too small is instead better to prune the vessel ($C \to 0$)
- the dynamics is governed by the wall shear stress and the system is in equilibrium ($\frac{\partial}{\partial t} = 0$) when the latter is uniform

Typically, the dynamical process is divided into two phases: initialization and adaptation. During the initialization phase, the organism forms the primitive structure of the network before it becomes fully functional. Subsequently, when the network commences resource transport, an adaptation process comes into play, facilitating further optimization. All these ideas are motivated by a set of experimental observations. Just as a notable example we can refer to the slime mold *Physarum polycephalum* study that has gathered a lot of attention in last years [8] [31] [30] [32](Fig. 2.5).

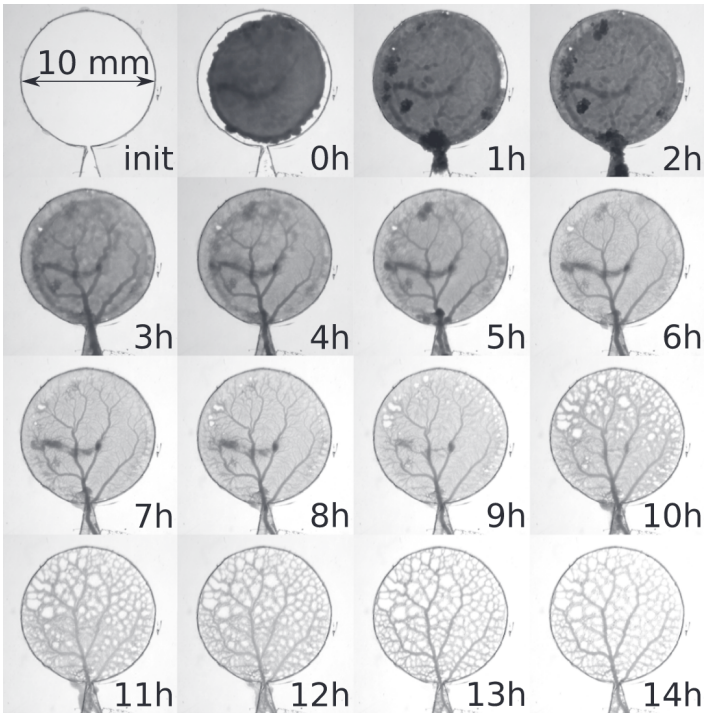

Figure 2.5: Time images following the development of a venation network by Physarum mold [8]. Note that some food is placed out from the circular domain and the network develop in order to evacuate the area and seek the resources.

Physarum is a slime mold that was shown to be able to react dynamically to the environment, forming a transport network, in order to find the most favorable way to seek food (Fig. 2.5). More in general it has been observed that, this adaptation process can lead to optimization and even vessel pruning in a variety of biological networks [33] [25] [34]. Furthermore, from experimental observations it also emerges that, under the pressure of natural selection, living systems have evolved diverse mechanisms to optimize the total energy consumption for mass transportation. In the context of plants, the structural optimization of the network primarily occurs during the initiation process, owing to the confinement of cells that cannot move freely. In contrast, animals predominantly achieve structural optimization through the adaptation process. Notably, endothelial cells from pruned vessels can be reused to form new vessels, facilitating dynamic adjustments.

Despite the distinctions between the two approaches we have outlined, i.e. cost optimization and dynamical adaptation, they can be integrated into a unified model when we incorporate the gradient flow of total energy cost into the adaptation dynamics. In simpler terms, it can be demonstrated that, during the process of adaptation dynamics, there is always a reduction in a globally defined energy cost.

Therefore, even within the dynamic approach, the core objective is, in fact, the minimization of a specific cost. More precisely, we can select the function F in equation (2.7) in such a manner that this implicit cost aligns with the cost function of the previously discussed optimization approach. In this scenario, both descriptions lead to identical outcomes. The optimal network structures are ultimately achieved as the adaptation dynamics steady states.

Remark 1. *It's worth emphasizing that this adaptation process, which is guided by the gradient flow and local stimuli, concord remarkably well with experimental observations. Despite that, this macroscopic dynamic process is influenced exclusively by macroscopic signals, such as wall shear stress in blood vessels. The underlying cellular mechanisms responsible for driving this adaptation remain hidden within this broader framework.*

Remark 2. *It is important to highlight that, the selection of the ansatz dynamics (2.7) in a manner that it aligns the adaptation description precisely with the optimization approach, is quite natural. The underlying principles that typically inform the choice of a particular dynamics rule (discussed previously) are fundamentally equivalent with the principles governing both local and global optimization within the alternative framework.*

Chapter 3

A unified model for discrete optimal networks

In the last chapter we briefly summarized the extensive literature of Optimal Channel Networks (OCNs), by reviewing the fundamental ideas that have been explored during time and acknowledging the contributions of major authors. Now, we are prepared to get to the heart of this thesis by starting to present in what consisted our research. The first goal that we tried to achieve was the description of a comprehensive model for optimal networks. Our aim was to propose a model able to include different cases already discussed in literature and possibly to explain new scenarios. Despite the fact that our idea was to provide a generalized picture, we still had to consider a minimum set of initial assumptions. In particular, we set as ground hypothesis that we are always dealing with:

- discrete networks on a 2D cubic lattice geometry
- single inlet networks
- a stationary regime ($\frac{d}{dt} = 0$)

The discrete formulation of the optimal transport problem we considered, can be simply stated as following:

given a set of N points that either require or furnish a resource, what is the optimal design for a network able to connect them in a way to fulfill all the requirements?

To answer this question it is fundamental to choose a geometry. Here with '*geometry*' we mean a graph where each node represent one of the N points requiring or supplying the resource and every edge is a possible channel connecting them. We will work always with a single inlet, meaning that there is a single node (source)

in which a positive flux of resources s_0 enter the system. On the other hand all the others nodes (sinks) have to be supplied by an homogeneous amount of flux $s_i = -\frac{s_0}{N-1}$. Therefore we will work with boundary conditions represented by the vector of load requirements $\{s_0, s_1 = -\frac{s_0}{N-1}, ..., s_N = -\frac{s_0}{N-1}\}$. The resource (for example water, blood, sap) flows in the channels following hydrodynamic rules in a stationary regime. The final optimal network will be a connected subgraph of the chosen geometry. Note that when constructing this subgraph we should always take all the N nodes but instead each link (channel) can be either taken or not, as well as the final network is connected.

We considered a 2D cubic lattice geometry (Fig. 3.1).

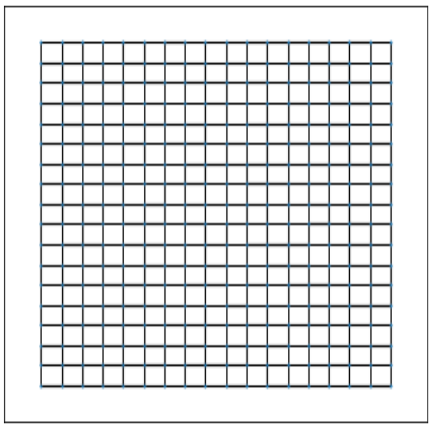

Figure 3.1: 18x18 square grid, each node represent an inlet, outlet or bifurcation of the network whereas every link is a possible channel

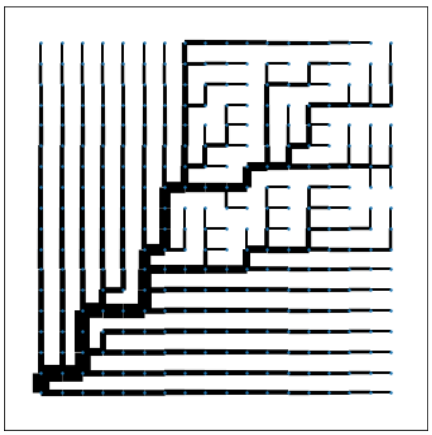

Figure 3.2: Example of a transport network with 2D cubic lattice geometry

Instead in Fig. 3.2 it is displayed an example of channel network realized on the selected 2D cubic geometry. Note that in general it exists a huge number of channel structures able to link all the nodes in a given geometry and to fulfill their loads requirements. But, in order to speak of '*optimal networks*' it is necessary to define a cost function, i.e. a performance measure for nets. In fact, only after having established a proper metric we can proceed to compare various channel designs and to discriminate between different degrees of optimality. Nevertheless, before starting to think at the actual form of the cost function, we will start the following discussion by providing a complete mathematical description of channel networks.

3.1 The space of feasible networks

In this section we will try to build a rigorous mathematical description for OCNs. Moreover, we will describe all the equations that rule their dynamical functioning and we will discuss some general analytical properties related to flows distributions inside channel networks. The initial question that we are treating is the following:

What is the space of parameters in which it is embedded every feasible network?

If our goal is to characterize a space in which every point represent exactly one network, we can just start from the geometric properties describing each edge. Let's say that all the geometrical properties of the *i-th* edge can be described by the vector $\bar{q}_i$. Then every network can be represented exactly as a vector $\bar{q} = \{\bar{q}_i\}$, encoding all the information about every edge. In the most simple case we can consider networks of smooth cylindrical pipes. In this case $\bar{q}_i = (r_i, l_i)$, where r_i and l_i are respectively the radius and the length of the i'th edge. In order to simplify as much as possible our discussion we will furthermore consider $l_i = 1, \forall i$. Therefore, $q_i = r_i$, i.e. every edge is uniquely defined by his radius, and a particular network can be identified simply as a vector of radii $\{r_1, r_2, r_3, ..., r_{N_{edges}}\}$.

It's worth noting that networks capable of meeting the loads requirements at each node are either spanning trees of our lattice or connected loopy networks that traverse each node (Fig. 3.3). This implies that the space of all feasible networks Ω can be represented as a subset of the space of all possible radii $\Omega' : R^{N_{edges}}$. Where a feasible configuration is just a configuration that link all nodes (Fig. 3.4).

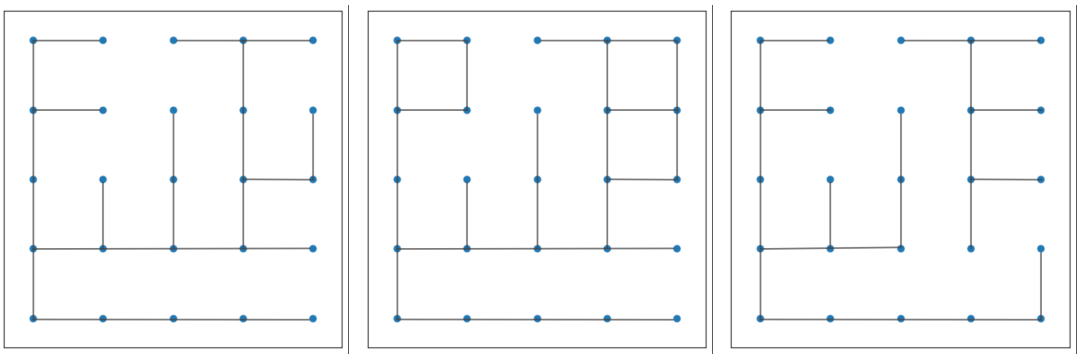

Figure 3.3: Examples of transport networks: (a) Tree, (b) Loopy network, (c) Unfeasible network.

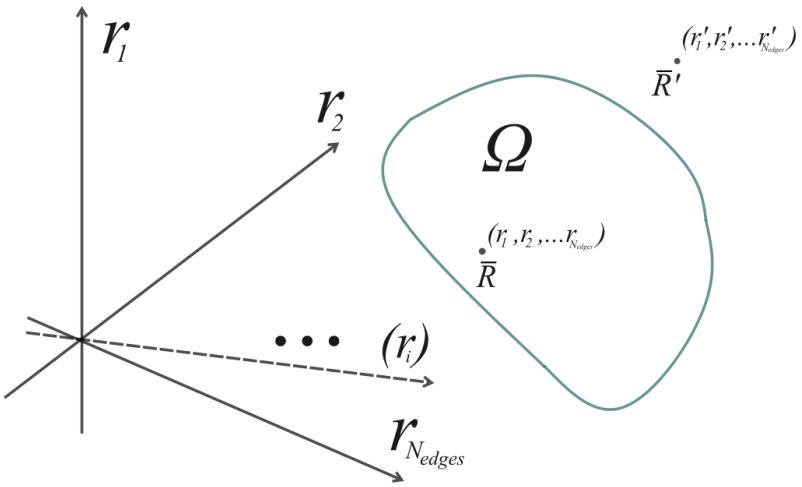

Figure 3.4: Illustrative representation of the radii space, R is a feasible network whereas R' is a disconnected one

Importantly, for every network in Ω we are always able to assign some fluxes at each edge in order to fulfill the load requirements $\{s_i\}$. This distribution of flows depends on the dynamical regime in which we are operating but is than unique for each configuration. The existence and uniqueness of a flow distribution is an issue of fundamental importance. Before going in depth into it we need to define the notion of conductance.

3.1.1 The conductance

If we consider only small radii, the Reynolds number is sufficiently low and the flow in the tubes can be well approximated by the Poiseuille flow:

$$v(r) = \frac{\Delta P}{4\mu L}(R_0^2 - r^2) \tag{3.1}$$

where μ is the viscosity of the fluid, ΔP the pressure drop, L the tube length, and R_0 the tube radius. In this case the volumetric flow rate $Q = 2\pi \int_0^{R_0} v(r) r \, dr$ can be written as:

$$Q = \frac{\Delta P \pi (2R_0)^4}{128 \mu L} \tag{3.2}$$

the resistance R of a pipe and the conductance C, are than naturally defined as:

$$R = \frac{\Delta P}{nQ} = \frac{128 \mu L}{n \pi D^4} = \frac{1}{C} \tag{3.3}$$

where n can be introduced to account for the possibility of parallel tubes bundles (Fig. 3.5).

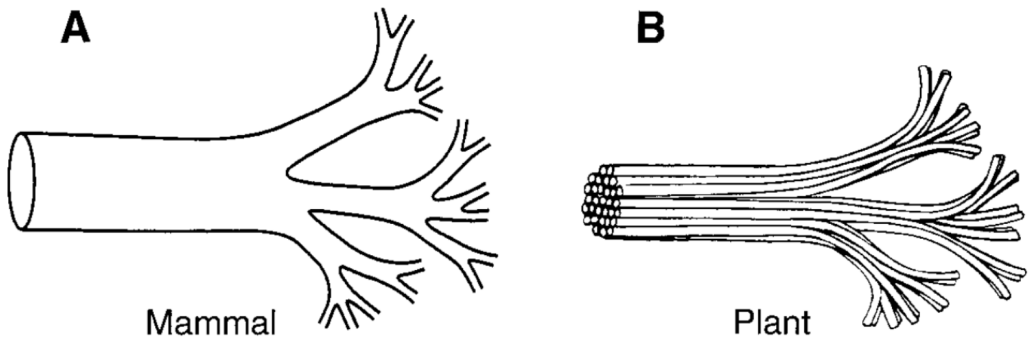

Figure 3.5: Structure of different biological transport networks. (A) Vascular network in mammals, (B) xylem channels in plants.

For blood vessels, n is usually equal to 1, whereas for vessels in plants such as leaf veins, n is greater than 1. In the following we will consider *n=1* without any loss of generality. In this regime the flows are thus characterized by:

$$Q = C(r)\Delta P, \qquad laminar flow \tag{3.4}$$

where we wrote $C = C(r)$ to stress that, once the properties of the fluid are known and considering our $L = 1$ setting, the conductance is essentially a function of the radius. So, the conductance is well defined for laminar flow but what happens if we go towards other regimes? Let start by recalling that in general the pressure gradient can be written as:

$$\Delta P = \lambda \frac{\rho}{4\pi^2} \frac{Q^2}{r^5} l \tag{3.5}$$

where ρ is the density and λ (called f in famous Moody's work, 1944 [35]) is the dimensionless friction coefficient, and can be written as:

$$\lambda \propto \left(\frac{r}{Q}\right)^k \tag{3.6}$$

in order to be concise we omitted the proportionality constant that depends only on the roughness of the tube and on the Reynolds number. Instead what is truly important for us is the behaviour of k. Importantly k is constrained in the range $0 \leq k \leq 1$. A value of $k = 1$ corresponds to laminar flow. As the shift from laminar to turbulent flow occurs, k continuously diminishes, reaching $k = 0$ in the case of completely turbulent flow. From (3.5) the flow dynamical equation (3.4) now reads:

$$\begin{aligned} Q &= C(r)\Delta P^{\alpha} \\ \alpha &= \frac{1}{2-k} \end{aligned} \tag{3.7}$$

where the flow in a tube is now a non linear function of the pressure gradient with an exponent α that range from 1 (laminar flow) to 1/2 (completely turbulent flow). The latter allow to define the conductance even out of the simple laminar flow as:

$$C(r) = K_C r^{3\alpha+1} \tag{3.8}$$

where K_C is a constant and (3.8) highlights the power law dependence on r.

3.1.2 Possible flow distributions

Following the definitions established in last section, we can say thet given a flow regime and particular fluid properties, there is a bijective mapping between radii and conductances. Therefore, for any given configuration $\{r_1, r_2, r_3, ...r_{N_{edges}}\}$, we are always able to find a unique configuration $\{C_1, C_2, C_3, ...C_{N_{edges}}\}$. This implies that given the radii, we can compute the conductances at each edge and then use the characteristic flow equation of the system to fix fluxes. Regardless of the flow regime, we can always adjust the pressure gradients to achieve a distribution of fluxes that satisfies the local load requirements $\{s_i\}$. While doing that, in order to generate a valid flows distribution, we must take care that three sets of equations holds:

$$\begin{cases} \sum_{j \in N_i} Q_{ij} = s_i & ,\forall i \\ \sum_{ij \in loop_k} \Delta P_{ij} = 0 & ,\forall k \\ Q_{ij} = C_{ij} f(\Delta P_{ij}) & ,\forall (ij) \end{cases} . \tag{3.9}$$

where N_i is the set of neighbours of node i (Fig. 3.6), $loop_k$ is the *k-th* independent loop in the network and note that here we introduced the double index notation *(ij)*. In this case the indices *(ij)* refer to the edge that link the nodes i and j. Sometimes it is way more useful to use this notation, that is related directly to the nodes and is even directional, therefore in the following we will use both the double and single index notations in order to label edges, but we will always make clear our choice. The first set of equation represent in (3.9) a continuity constraint for each node. The second relation is the set of Kirchoff's equations that assure we are constructing loops in accord with a valid pressure field $\bar{P}$. Finally the last group of equations are the dynamical flow equations we discussed in previous section.

Let's now prove some interesting properties about this distribution of fluxes that will come usefull later.

Lemma 1. *Given a set of conductances $\{C_1, C_2, C_3, ...C_{N_{edges}}\}$ and a vector of load requirements $\{s_1, s_2, s_3, ...s_{N_{nodes}}\}$ for a connected network in laminar regime, the distribution of flows $\{Q_1, Q_2, Q_3, ...Q_{N_{edges}}\}$ satisfying (3.9) exists and it is unique.*

Proof. To prove it we can show that the valid distribution of flows is the unique solution of a linear system of equations. Remember that if we have a set of k linearly independent equations for k unknown then the solution is proven to exist and to be unique. For a network of N nodes we have N linear continuity equations that must hold. However only *N-1* are linearly independent, the reason of that if the additional property that the total current flowing in the system must be a constant. If the network is a tree then $N_{edges} = N - 1$, thus in this case we have

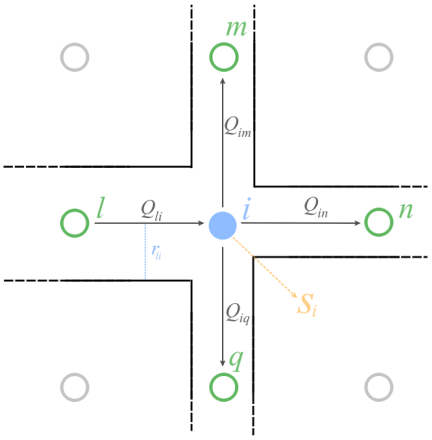

(a)

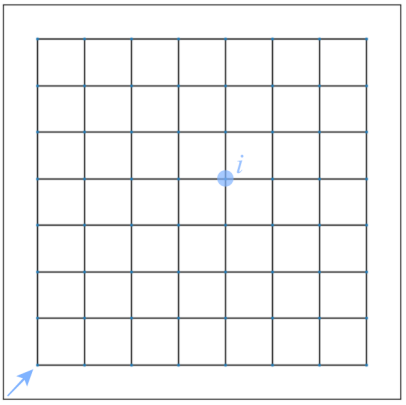

(b)

Figure 3.6: Schematic of a network. (a) Close view on a bifurcation, note that here $N_i = \{l, n, m, q\}$, s_i is the outlet at node i and at each node is defined a pressure $P(i)$. (b) Full view of a small network, where generally we consider a inlet flux of resource at the bottom left node and an homogeneous distribution of outlets elsewhere. Note that each node i can have at most 4 neighbours.

$N-1$ variables (ΔP_i) and exactly $N-1$ linearly independent constraints, there is therefore only one solutions for $\Delta\bar{P}$. For every independent loop we add to the network the number of variables grow $N_{edges} = N - 1 + n_{loops}$. But at the same time for every such loop we have an independent Kirchoff's (linear) equation to satisfy. So at the end even in this case the only valid solution $\Delta\bar{P}$ is the output

of a linear system of equations of size $N_{edges} = N - 1 + n_{loops}$. We can end our proof just observing that for a set of conductances $\bar{C}$ and the unique solution for pressure gradients $\bar{\Delta P}$, flows can than be uniquely determined via the flow dynamical equation (3.9). □

If we consider instead a turbulent regime the system of equations we have to solve in order to fix the flows become non-linear. In general the behaviour of non linear systems is quite complex. Luckily, exploiting the increasing monotonicity of the dynamical flow equations, we can use the results developed by Duffin [36] for non-linear resistive networks. The latter assure that the existence and uniqueness of a solution for the flows can be generalized also to the turbulent case.

Lemma 2. *If the network is a tree the unique solution depends only on the tree structure and not on the exact values of each conductance.*

Proof. We can prove it straightforwardly just by observing that if the network is a tree the linear system that determines the unique solution for the flows can be written only using the continuity equations at each node. Thus the linear system do not depend in any way to the conductances values but only on the connection pattern. We can alternatively prove it by induction starting from the leaves of the tree and showing that at any point the flux entering a node depends only on the entering fluxes. □

We can now end this section with some summary remarks.

Remark 1. *For a given geometry (lattice), every feasible network can be represented as a radii vector:* $\{r_1, r_2, r_3, ...r_{N_{edges}}\}$

Remark 2. *Given the flow regime and the specific fluid properties (or the properties of whatever is flowing), we can map each net from the radii space to the conductance space. Each network is thus uniquely represented by:* $\{C_1, C_2, C_3, ...C_{N_{edges}}\}$

Remark 3. *For each tree network, there is a unique feasible solution for the fluxes that does not depends on the conductances values but only on the linkage pattern of the tree.*

Remark 4. *For loopy networks, there is always a unique solution for the flows at each edge and it depends on the specific values of the conductances* $\bar{C}$.

Remark 5. *The above discussion began with the assumption of cylindrical pipes on a homogeneous lattice, but this hypothesis can be relaxed in order to account for more complex scenarios. If we are willing to do that, we can simply replace 'r' with other geometric parameters of the edges such as hydraulic radius and allow for non-uniform lattice spacing.*

3.2 The cost function

To find a good model for the cost function, describing network 'optimality', is a pivotal point of this research field. During the last century of studies several proposals have been presented. However, after a wide analysis of the literature, we developed the idea that all those models had more similarities than differences. We than tried to propose a general model able to summarize the efforts previously done on OCNs. In this section we will present our proposal. The latter seems to be able to well explain a lot of the previous models. Furthermore we hope that this description could help to establish a clear and modern picture of the OCNs problem, revealing some new insights and promising for interesting future developments.

3.2.1 Formulation in terms of conductances

In order to build such kind of general model we have to understand well what are the key ideas about OCNs that can be find transversely in the literature. Perhaps, one of the most crucial aspects that every formulation must address, is the establishment of a performance measure for networks. To start, we can say that the standard assumption on the cost function is that it can be written as the sum of two terms:

$$J = J^{(D)} + J^{(\gamma)} = \sum_{ij} [Q_{ij} \Delta P_{ij} + b C_{ij}^{\gamma}] \tag{3.10}$$

here $J^{(D)}$ represent the sum of the energies, per unit time, needed to sustain the flows at each edge, while $J^{(\gamma)}$ is the cost necessary to physically build and sustain the network. Note that here we used the double indices *(ij)* to label edges and b is a dimensional constant that in the literature is frequently addressed to as *metabolic constant*. This shape for the cost function, although being quite arbitrary, has a very intuitive meaning. The fact to consider as first term the energetic cost needed to simply 'make work' the net is clearly the most natural thing to do, and, on the other hand, it is easy to see that considering this term alone would lead only to naive considerations. In general, if the conductance C_{ij} increases, it allows the same flow Q_{ij} to be achieved with a smaller pressure gradient ΔP_{ij}. This implies that, without a penalty ($J^{(\gamma)}$) for enlarging the pipes, the optimization problem would naturally lead to constructing the largest possible network, as it can be graphically understood looking at Fig 3.7.

Alternatively, another approach is to consider only $J^{(D)}$ as the cost function while introducing a global constraint related to limited resources in the system, i.e. $J^{(\gamma)}$=cost. Both methods yield similar conclusions. For now, we will proceed with the unconstrained formulation and we will revisit the comparison later.

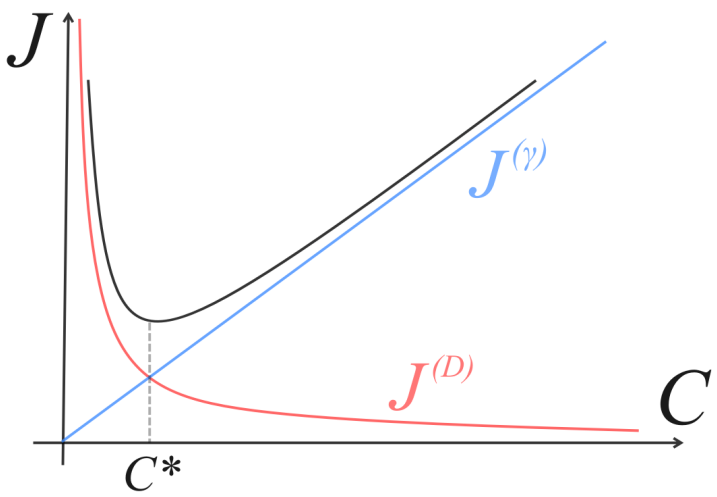

Figure 3.7: The cost function for a single edge as a function of his conductance C. Note that the current passing through the edge is fixed and $\gamma = 1$.

Now, since we know that every network is represented as a conductances vector, we can write the dissipation term $J^{(D)}$ in term of conductances depending on the dynamical regime in which we are operating. We can do that by using the general form of the dynamical flow equation (3.7). The dissipation, in a general case, therefore reads:

$$J^{(D)} = \sum_{ij} Q_{ij}^{\frac{\alpha+1}{\alpha}} C_{ij}^{-\frac{1}{\alpha}} \tag{3.11}$$

then, by considering all together, the final cost function can be expressed as:

$$J = \sum_{ij} [Q_{ij}^{\frac{\alpha+1}{\alpha}} C_{ij}^{-\frac{1}{\alpha}} + bC_{ij}^{\gamma}] \tag{3.12}$$

note that the latter is able to describe every hydraulic flow regime between the laminar-turbulent transition and can account for a wide range of conductance costs $J^{(\gamma)}$ as well. Additionally, this model extends its applicability to other flow scenarios, including those involving non-Newtonian fluids, pulsatile flow, plug flow, heat and electrical flows, and 1D Fick's diffusion (mass flow). In these instances, it is essential to recognize that equation (3.8) may not maintain its validity. The relationship between conductances and radii needs to be adjusted to account for the specific physics of each process. Nevertheless, in the mentioned cases, we can still assume a power-law dependence, expressed as $C(r) \propto r^m$.

3.2.2 Formulation in terms of radii

An alternative formulation, often present in the literature, is to write the cost using the radii, as $J = J(\{Q_{ij}\}, \{r_{ij}\})$ instead of $J = J(\{Q_{ij}\}, \{C_{ij}\})$. We can easily modify (3.12) to achieve such description by recalling (3.8). We thus have:

$$J \propto \sum_{ij} [Q_{ij}^{\frac{\alpha+1}{\alpha}} r_{ij}^{-\frac{3\alpha+1}{\alpha}} + b' r_{ij}^{(3\alpha+1)\gamma}] \tag{3.13}$$

from this formulation the second term, related to the metabolic cost of a channel, is expressed directly as a function of its geometrical dimension. Note that if γ can be chosen freely in order to account for different type of constraints, instead the overall exponent of the second term depends on the specific flow regime in which the network is operating. This aspect is crucial. In general, the selection of γ may seem quite arbitrary. Writing the maintenance energy cost of a pipe with conductance C_{ij}, as C_{ij}^{γ}, appears reasonable, but connecting the exponent γ with real scenarios can be challenging. This is why, especially in seminal papers, the maintenance cost is frequently expressed in terms of the radius (as in eq. 3.13). In fact, through the radii description, it is then easier and more intuitive to justify an exponent in the second term of the cost function. One can for example argue that such maintenance cost is proportional to the volume of a pipe [3], or to his cross section [37], i.e. respectively $(3\alpha + 1)\gamma = 2, 1$.

So we have seen that using the formulation in terms of radii it is more easy to gather some intuition about the meaning of a particular choice for the term $J^{(\gamma)}$ and this will lead to some interesting consequences in the following (Sec. 3.4.1). As last comment, let's just observe that instead, in both formulations, the dissipation term $J^{(D)}$ can be nicely represented graphically [38]. The idea is to construct a schematic as the one represented in Fig. 3.8 for a simple 4 nodes network. Note that each vertical line represent a bifurcation and the construction procedure is wisely designed in a way that the constraints (3.9) are geometrically enforced. Kirchoff's equations for the pressure gradients ΔP_i are naturally satisfied if the left and right sides of the full figure have the same length. Similarly, the continuity equation at each node are enforced by preserving the total section of the picture. At last, the dynamical flow equations at each edge are represented inside each white rectangle and are naturally fulfilled by construction. In the laminar regime observe that the slopes of the rectangle diagonals represent the resistances $(1/C)$ of each edge. The interesting graphical property of this kind of schematics is that now the dissipation cost $J^{(D)}$ assume the interpretation of an area, i.e. the sum of white rectangle areas in Fig. 3.8. Furthermore one can even think that all the possible configurations of the network are now represented by all the possible ways in which we can strain the whole schematic while preserving his rectangular shape. This is even another way to see the effect of to do not consider a price for conductances. In fact it is

easy to see that if we send all $C_i \to \infty$ the slopes of all the diagonals go to 0 and graphically the white area representing the cost vanishes too. Finally, note that such schematics can be easily built even in a turbulent flow regime, one just have to consider that the flow dynamical equation will change (Fig. 3.8). Thus even in turbulent flow we can provide this intuitive graphical interpretation of $J^{(D)}$.

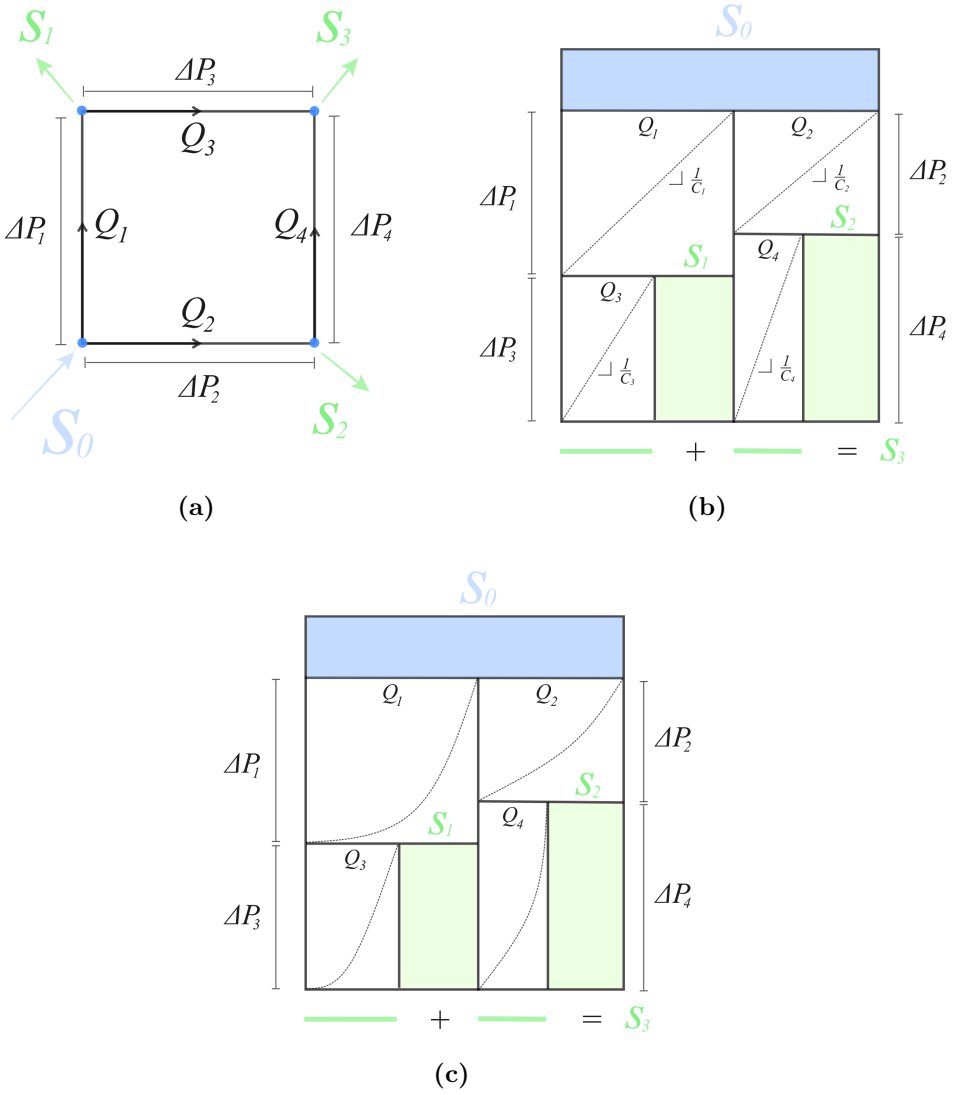

Figure 3.8: (a) 4 node network, (b) geometrical construction that represent the 4 nodes network in laminar flow, (c) geometrical construction that represent the 4 nodes network in turbulent flow

Remark 1. *Note that all this discussion started from an ansatz on the form of the cost function. We wrote it as the sum of two contribution, $J^{(D)}$ and $J^{(\gamma)}$. In principle one can add other terms attempting to describe more sophisticated effects. For example one could add an energetic cost due to turbulent dissipation on bifurcations or a term lowering the cost for networks that are able of perform an efficient diffusion at lower scales. Nevertheless (3.12) seems to us the simplest and most intuitive 'minimal model' that can be adopted. For this reason, as suggested by the Occam's razor, we believe that the core principles of transport nets can be well captured in this framework without adding other extravagant assumptions.*

Remark 2. *Note that both for trees and loopy networks the cost depend uniquely on the conductances, the fluxes being automatically fixed by load constraint as shown in section 3.1.2.*

Remark 3. *The equivalent formulation of the model with a global constraint approach would be:*

$$J = \sum_{ij} Q_{ij}^{\frac{\alpha+1}{\alpha}} C_{ij}^{-\frac{1}{\alpha}}, \;\; K = \sum_{ij} C_{ij}^{\gamma} \tag{3.14}$$

where K represent the amount of resources available in the system to build the network.

3.3 The optimization problem

Now that we have established a model, we can finally compare networks. The important question that naturally arises is:

What are the stationary points of our model and what does influence their stability properties in the space of feasible networks?

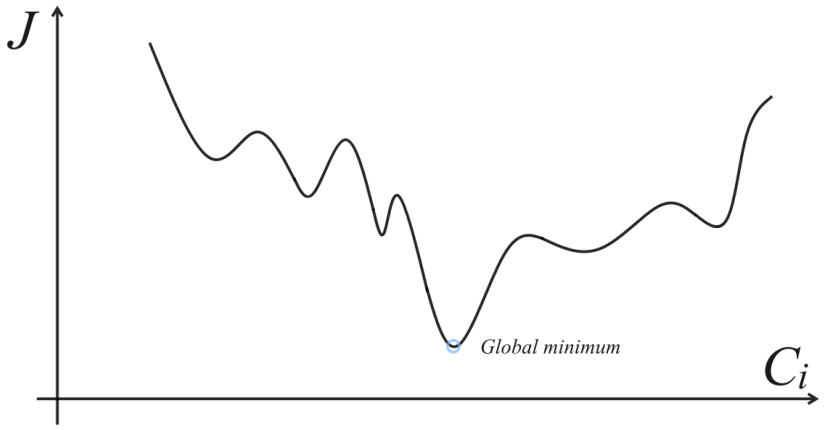

Figure 3.9: Schematic of the cost landscape

We are interested in these points because we operate on the assumption that our model (3.12) effectively captures the performance of different networks. Therefore, the absolute minimum will represent the best network that we can possibly describe. The latter is usually referred to as the *principle of global optimization*. Furthermore, model (3.12) features a very complex landscape of local minima (as displayed for providing a qualitative intuition in Fig. 3.9). These points are interesting as well since, in many cases, reaching the absolute minimum is unlikely, and the truly relevant issue is the overall behavior of the intricate minima landscape. Despite their relevance, the problem of determining all the minima of model (3.12) is quite challenging, and for this reason, the customary strategy is to resort to a second principle: the *principle of local optimality*. In the following section, we will present this principle and then we will show how to employ it in order to obtain fundamental information about the behavior of the cost minima.

3.3.1 The local optimization

The most intuitive approach to the presented problem is to start by imposing the stationarity of (3.12) with respect to conductances C_{ij}. Note that, since the

conductances are decoupled, this minimization leads to a set of local (one for every edge *ij*) stationarity constraints of the type $C^*_{ij} = f(Q_{ij})$. For this reason, we will refer to this step as 'local optimization' from now on. The result is:

$$C^*_{ij} = A_c Q_{ij}^{\frac{\alpha+1}{\alpha\gamma+1}} \tag{3.15}$$

$$A_c = \frac{1}{\alpha\gamma b}^{\frac{\alpha}{\alpha\gamma+1}} \tag{3.16}$$

this relation holds for every conductance independently, meaning that we can build a global stationary point by considering a network for which (3.15) is enforced at each edge, explicitly:

$$\bar{C^*} = (C^*_1, C^*_2, ..., C^*_{N_{edges}}) \tag{3.17}$$

we can then proceed with the second derivative analysis:

$$\frac{\partial^2 J}{\partial C^2_{ij}} = \frac{1-\alpha}{\alpha^2} Q_{ij}^{\frac{\alpha+1}{\alpha}} C_{ij}^{-\frac{1}{\alpha}-2} + b\gamma(\gamma-1)C_{ij}^{\gamma-2} \tag{3.18}$$

since C_{ij} and Q_{ij} are always positive (to compute dissipation we take all currents in the positive sense) and $\alpha \leq 1$, the only way to get (3.18) to be ≤ 0 is to take $0 \leq \gamma \leq 1$. However, even in this case one obtain that at the stationary point the second derivative (3.18) is always positive. At the end, we can conclude that indeed (3.15) describe always minima.

Nevertheless, we have to be very careful to interpret this result. In fact during all this derivation we considered fixed flows. Therefore, the above characterization of the local minima, holds only if we are able to change the values for the conductances without affecting the flows Q_{ij}, but this is in general unfeasible. One can think to redo the computations considering simply $Q_{ij} = Q_{ij}(C_{ij})$ in order to account to the fact that also currents change in response to conductances fluctuations. But again this is problematic since the currents change in a non-trivial way in order to fulfill equations (3.9). In particular, it is easy to see that the perturbation of a single conductance can affect all the currents in a loop, and thus it has furthermore a non-local effect that depends on the specific overall structure of the net, making this approach intractable. The difficulty to deal with this aspect in a straightforward way is exactly the reason why this point was always poorly discussed in literature, and often simply bypassed. What is instead commonly done it is to just assume that the optimal networks should satisfy (3.15) at every edge. This is exactly the mentioned *principle of local optimality*. The implications of considering this assumption are profound. In particular that allows to prove that the overall behaviour of the minima depends only on γ, as we will show in detail in

section 3.3.4. We tried to deepen our understanding of that issue, with the aim of providing a proof that the *principle of local optimality* is indeed unnecessary, as already implied by global optimality.

In Appendix A, we presented a methodology for precisely solving the problem in the case of a simple loop involving two channels. For this specific configuration, we achieved an exact and fully analytical solution, demonstrating that the stationary points (3.17) are indeed the unique local optima in the whole Ω domain, and their stability is solely dependent on γ. Notably, in this context, the application of a *principle of local optimality* is unnecessary, as we established that the local optimal constraints naturally align with the global optimality.

As we progress to more complex scenarios involving larger loops, the strategy outlined in Appendix A becomes progressively more and more cumbersome. Handling such situations may necessitate the assistance of numerical software, and the approach struggles to generalize results to any scale. In Appendix B we proposed a reasoning leading to the conclusion that, even enlarging the size of the possible loops, stationary points (3.17) maintain the usual stability properties driven by γ. However, we still fail to prove that in that scenario there are no other possible candidate local minima, and therefore, a conclusive proof that the *local principle of optimality* is always exactly coming from the global one remain elusive.

Before concluding this section, let's consider some important implications of stationary points (3.17). In fact, if we recall that it exists a power law dependence between conductances and radii (3.8), the stationarity constraints can be expressed even for each radius:

$$C_{ij} \propto r_{ij}^{m} \tag{3.19}$$

$$r_{ij}^{*} \propto Q_{ij}^{\frac{\alpha+1}{m(\alpha\gamma+1)}} = Q_{ij}^{\epsilon} \tag{3.20}$$

where (3.19) is the more general version of (3.8), holding for a wide range of physical transport flows. Relation (3.20) is very insightful and it represents a generalization of the Hess-Murray's law. In particular if we substitute the ansatz of Murray ($\alpha = 1, m = 4, \gamma = 1/2$) we get exactly $\epsilon = 1/3$, in accord with his findings [3]. Moreover, we can substitute the latter in the continuity equation for the flows at a bifurcation and we find:

$$r_0^{\frac{1}{\epsilon}} = \sum_k r_k^{\frac{1}{\epsilon}} \tag{3.21}$$

here, r_0 denotes the radius of the parent vessel, while r_k refers to the radii associated with the channels originating in the bifurcation. Therefore, ϵ plays a crucial role in determining the local branching characteristics of the network, representing a truly meaningful parameter.

3.3.2 The global optimization

By embracing the principle of local optimality, i.e. restricting the feasible networks to those defined by (3.17), we can dramatically reduce the space of configurations to take into account. It's noteworthy that the local optimal constraint is trivially fulfilled for $(Q_{ij}, C_{ij}) = (0,0)$, allowing every conceivable connected linkage pattern to be a minimum. In this scenario, we can still find some ulterior general properties, on the behavior of local minima, by prosecuting on an analytical path. In fact, if we substitute the constraint (3.15) inside our model (3.12), we are able to write the total cost of a network as a function of the currents alone:

$$J = A_J \sum_{ij} Q_{ij}^{\frac{\alpha\gamma+\gamma}{\alpha\gamma+1}} \propto \sum_{ij} Q_{ij}^{\Gamma} \tag{3.22}$$

$$A_J = [A_c^{-\frac{1}{\alpha}} + bA_c^{\gamma}] \tag{3.23}$$

note that $\gamma > 1 \iff \Gamma > 1$ and vice versa. This is particularly valuable, especially considering that for such models, Banavar has already provided robust analytical results [18].

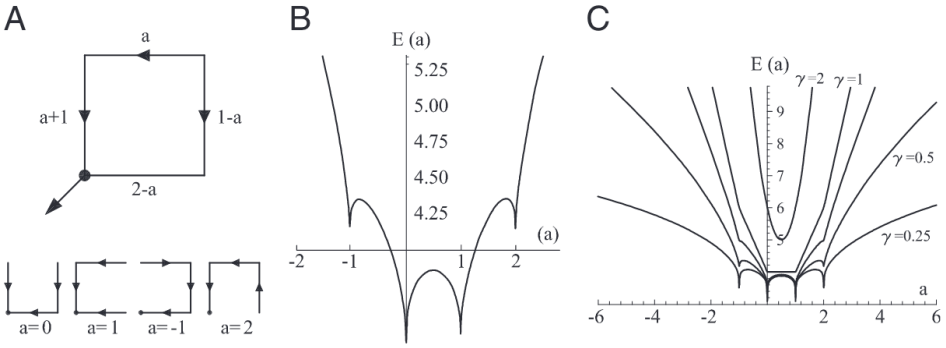

Figure 3.10: Schematic for a four node network [39]. (A) The four-node arrangement, with indications on the currents that respect continuity (note that a unit flux is injected at each node). The dot is the outlet. Here, the current a is taken as the parameter regulating the entire distribution of fluxes owing to continuity. (Lower Left) The only loopless configurations of the system are generated by integer values of a: possible trees correspond to the cases $a = 0, -1,1,2$. (B) Plot of the function E vs. a from $E = |a|\gamma + |a+1|\gamma + |1-a|\gamma + |2-a|\gamma$ (with $\gamma = 0.5$), which is derived by computing energy dissipation after implementation of continuity at the nodes. In particular, the plot of $E(a)$ highlights that there are local minima in correspondence with one of the four currents being zero ($a = 2,1,0,-1$), corresponding to the four trees shown in Lower Left. (C) Energy functions $E(a)$ for the cases $\gamma = 0.5,0.75,1,2$.

Specifically, when $\Gamma > 1$, the absolute minimum is clearly defined and, as demonstrated by Banavar, corresponds to a fully looped network. On the other hand, if $0 < \Gamma < 1$, all the spanning trees of our geometry are local minima and the exact global minimum is difficult to characterize. To understand better this result we can look at Fig. 3.9 illustrating the situation in the simple case of a four nodes network. This is indeed the ultimate analysis that one can perform from an analytical point of view. We should now just manually compare the minima looking for the absolute one. Unfortunately the number of local minima grows exponentially with the dimension of the domain, meaning that from now on the accuracy of our results, and in particular the location of the absolute minimum, depends on the quality of the numerical methods we use to navigate into such exponentially growing space.

3.3.3 The constrained formulation

Let's take a look at what would have been the result if we had work with the constrained problem (3.14). Skipping the minimization steps (performed using the Lagrange multipliers), we would have find:

$$\left[\begin{array}{l} J^{(constraint,*)} = A_J^{(constraint)} \sum_{ij} Q_{ij}^{\frac{\alpha\gamma+\gamma}{\alpha\gamma+1}} \\ \implies J^{(constraint,*)} \propto \sum_{ij} Q_{ij}^{\Gamma} \end{array}\right. \tag{3.24}$$

$$\left[\begin{array}{l} C_{ij}^{(constraint,*)} = A_c^{(constraint)} Q_{ij}^{\frac{\alpha+1}{\alpha\gamma+1}} \\ \implies r_{ij}^{(constraint,*)} \propto Q_{ij}^{\frac{\alpha+1}{m(\alpha\gamma+1)}=\epsilon} \end{array}\right. \tag{3.25}$$

therefore, we obtain equations analogues to the unconstrained problem with the same exponents (Γ, ϵ). This means that the global properties of the landscape of minima do not change in the two approaches. Nevertheless, the two problem are exactly equivalent only if the proportionality constants $(A_c, A_J) = (A_c^{constraint}, A_J^{constraint})$ coincides. We can require that the scaling of conductances/radii is exactly the same by imposing:

$$\left[\begin{array}{l} A_c = A_c^{(constraint)} \\ \implies b = \mu \end{array}\right. \tag{3.26}$$

or instead we can require that the costs are exactly the same by enforcing:

$$\left[\begin{array}{l} A_J = A_J^{(constraint)} \\ \implies b = \mu[\frac{\alpha\gamma+1}{\alpha\gamma}]^{-(\alpha\gamma+1)} \end{array}\right. \tag{3.27}$$

where μ is the Lagrange multiplier that is employed in the constrained approach and is equal to:

$$\mu = \frac{K^{-\frac{\gamma\alpha+1}{\alpha\gamma}}}{\gamma\alpha}[\sum_{ij} Q_{ij}^{\frac{\alpha\gamma+\gamma}{\alpha\gamma+1}}]^{\frac{\gamma\alpha+1}{\alpha\gamma}} \tag{3.28}$$

However, (3.26) and (3.27) can't hold at the same time. This mean that model (3.12) and (3.14), even if closely related and sharing the same general behavior and properties, are therefore intrinsically different. Note that, if instead we propose a new model in the form:

$$J = \sum_{ij} [Q_{ij}^{\frac{\alpha+1}{\alpha}} C_{ij}^{-\frac{1}{\alpha}} + b' C_{ij}^{\gamma}], \;\; K = \sum_{ij} C_{ij}^{\gamma} \tag{3.29}$$

this new formulation can be exactly identified with model (3.12) just by considering:

$$\left[\begin{array}{l} b = b' + \mu \\ \mu = \frac{K^{-\frac{\gamma\alpha+1}{\alpha\gamma}}}{\gamma\alpha} [\sum_{ij} Q_{ij}^{\frac{\alpha\gamma+\gamma}{\alpha\gamma+1}}]^{\frac{\gamma\alpha+1}{\alpha\gamma}} \end{array} \right. \tag{3.30}$$

Let's end this section with some interesting remarks:

Remark 1. *At the end, we can wrap together our analytical findings by saying that all the overall properties of the local minima lanscape depends on the two exponents* (Γ, ϵ). *In particular for* $\Gamma > 1$ *the problem is completely solved and we are able to characterize the behaviour of the unique absolute minimum. Instead for* $\Gamma < 1$ *the absolute minimum should be searched numerically but we know that we have to look only between trees. In both cases the radius scaling and thus the branching properties of the network are described by* ϵ.

Remark 2. *From a theoretical point of view the framework we developed depends only on the two underlying principles of local and global optimality. Despite that, we should also recall that there are several other assumptions that come into play if we want to use this model in particular physical scenarios. Let's recall that for every specific application:*

1. *Even knowing exactly the flow regime (i.e.* α*) one still has to make an asatz on the form of* $J^{(\gamma)}$ *by choosing arbitrarly a value for* γ.

2. *The flow should be stationary and it should occur in cylindrical pipes on a uniform lattice geometry (i.e.* $l_i = 1, \forall i$*)*

3. *We should be able to express the flow in a pipe as a function of its radius and the* ΔP *in a factorized form* $Q = C(r) f(\Delta P)$. *Where the function depending on* r *is our definition of conductance whereas* f *is a power law.*

4. *Furthermore, even C(r) is a power law.*

5. *We should be able to write the power needed to sustain the flows as* $J^{(D)} = Q\Delta P$.

3.4 The strength of the model

Finally, we are ready to show all the interesting properties that arises from our unified description. As fist thing let's show that it is able to generalize successfully a variety of different proposals that have been advanced in the last century of research. As we emphasized earlier, the overall properties of a model essentially depend on the scaling exponents (ϵ, Γ). Conversely, our model describes a specific situation only when we set its parameters (α, γ, m). For instance, we can describe a laminar flow with a metabolic cost proportional to the volume by considering $(\alpha = 1, \gamma = 1/2, m = 4)$. To facilitate the comparison between the previous formulations and ours, the following table compiles the (ϵ, Γ) exponents predicted in the literature, followed by the specific cases that the authors considered, expressed in terms of the parameters of our model.

Literature review			
	$r \propto Q^{\epsilon}$	$J \propto \sum Q^{\Gamma}$	α, γ, m
Present work	$\epsilon = \frac{\alpha+1}{m(\alpha\gamma+1)}$	$\Gamma = \frac{\gamma(\alpha+1)}{(\alpha\gamma+1)}$	/
Murray [3]	$\epsilon = \frac{1}{3}$	/	$\alpha = 1, \gamma = \frac{1}{2}$ $m = 4$
Uylings [5]	$\epsilon = \frac{3}{7}$	/	$\alpha = \frac{1}{2}, \gamma = \frac{4}{5}$ $m = \frac{5}{2}$
Bohn [19] Katifori [21] Corson [20] Hu [25] Lonardi [22] Ronellenfitsch [29]	$\epsilon = \frac{1}{2(\gamma+1)}$	$\Gamma = \frac{2\gamma}{\gamma+1}$	$\alpha = 1, \gamma$ $m = 4$

	$r \propto Q^{\epsilon}$	$J \propto \sum Q^{\Gamma}$	α, γ, m
Durand [40]	/	$\Gamma = \frac{2n}{n+m'}$	$\alpha = 1, \gamma = \frac{2n}{m}$ $m = 2m'$
West [6]	$\epsilon = \frac{1}{2}$	/	$\alpha = \frac{1}{2}, \gamma = 1$ $m = 2$
Almeida [26]	/	$\Gamma = \frac{4}{3}$	$\alpha = 1, \gamma = \frac{1}{2}$ $m = 4$
Facca [23]	/	$\Gamma = 1$	$\alpha = 1, \gamma = 1$ $m = 4$

Moreover, our model seems to be the first that can fully account for the local and global properties of:

- the laminar-turbulent transition ($\alpha \in [1/2,1], m = 3\alpha + 1$)
- non-Newtonian fluids tubular flows ($\alpha = 1/\omega, m = 3 + 1/\omega$)
- heat conduction ($\alpha = 1, m = 2$)
- plug flow ($\alpha = 1, m = 2$)
- 1D Fickian diffusion (mass flow) ($\alpha = 1, m = 2$)

where ω is the degree of non-Newtonianity of a fluid. Among the latter, the possibility to describe the laminar-turbulent transition in particular open some interesting avenues. In the following sections, we will analyze two possible scenarios that can arise as a consequence of the interplay between (α, γ, m), specifically, in the laminar-turbulent situation.

3.4.1 The laminar-turbulent transition

In this section, we aim to explore the implications of considering a network with a laminar-turbulent transition taking place as the channel scale decreases. This choice is justified by the fact that the Reynolds number, dictating the flow regime, is dependent on the radius of the tube where the flow occurs. Smaller radii result in lower Reynolds numbers, favoring laminar flow, while larger tubes promote turbulence. Moreover, let's assume that we want to maintain a consistent geometric constraint as expressed in (3.13). This implies that the cost of maintaining an edge, with respect of its size, should keep the same behaviour across different scales of the network. To adhere to this assumption, we need to adjust γ to accommodate the effect of changes in flow regimes. For instance, if we aim to keep the maintenance cost proportional to the volume in various flow regimes, i.e. scales within the network, we must modify the exponent γ accordingly, as follows:

$$J^{(\gamma)} \propto r^{\gamma m} \tag{3.31}$$

$$\gamma = \frac{2}{3\alpha + 1} \tag{3.32}$$

where it should be recalled that for the turbulent-laminar transition $m = 3\alpha + 1$. We can clearly see that in laminar flow ($\alpha = 1$) the latter can be satisfied if $\gamma = 1/2$ (Murray). Instead in the case of completely turbulent flow ($\alpha = 1/2$) we get $\gamma = 4/5$ (Uylings). Therefore, by considering that the metabolic cost of a channel is proportional to its volume, γ change but remains always lower than 1. This is unable to provide a significant change in the branching behaviour. If instead we consider a more general scenario where we want to account for $J^{(\gamma)} \propto r^k$ we should consider:

$$\gamma = \frac{k}{3\alpha + 1} \tag{3.33}$$

notably, we than see that if $k > 5/2$ the exponent γ can go beyond 1 during the laminar-turbulent transition. This is very important. In fact if the system is working in a situation in which $k > 5/2$ then we can predict that at some scale γ will grow beyond 1, changing completely the characteristics of the network as shown in Fig. 3.11. This behavior represents a theoretical implication that could therefore manifest itself in practical scenarios, whether in natural systems or in the context of technological applications.

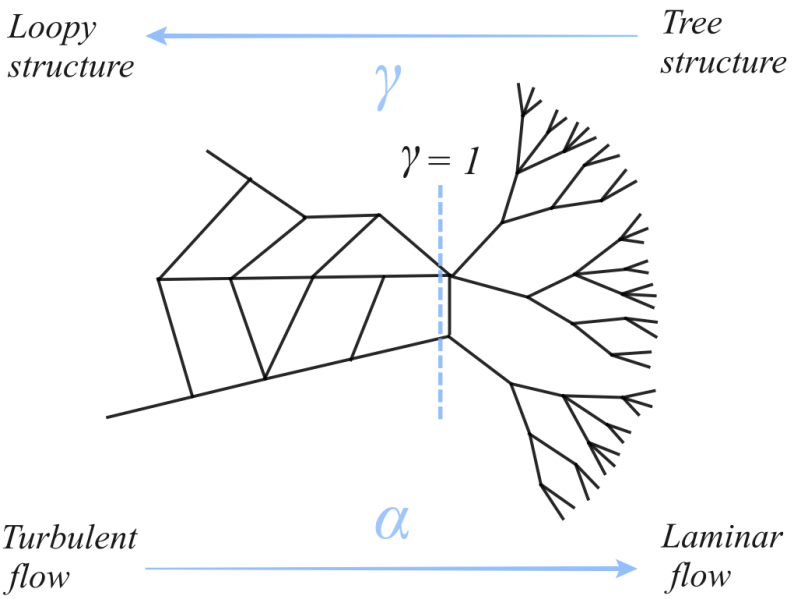

Figure 3.11: Bistable branching behaviour in a network featuring laminar-turbulent flow transition for $m > 5/2$

3.4.2 Expensive/Cheap channels transition

Another similar transitioning behaviour can be explained by analyzing the new degrees of freedom that our description can offer. In particular, let's think this time to consider a network working on a unique regime, for instance laminar. But now, we can force γ to vary along different scales as an effect of a variation in the metabolic cost of maintaining the channels. This is intuitively reasonable. We can for example think that, as the pipes becomes very thick, they develop a more expensive geometrical scaling. In this case we should write:

$$\gamma = \frac{k}{4} \tag{3.34}$$

where α is considered equal to 1 since we set the assumption of laminar flow and now is k that is changing with the scale of the network. When k become bigger than 4 the branching behaviour change as depicted before but in the opposite dependence with the channels dimension. This behaviour is exemplified in Fig. 3.12. In this case we see that the network develop a loopy structure when the channels are sufficiently small. Therefore the following phenomenological explanation could represent an additional tool to understand the functioning of biological networks where we see exactly this behaviour. Finally, one can also think that, the two

effects described in sections 3.4 and 3.4, can combine together furnishing a even richer description of possible transitioning behaviours across different scales.

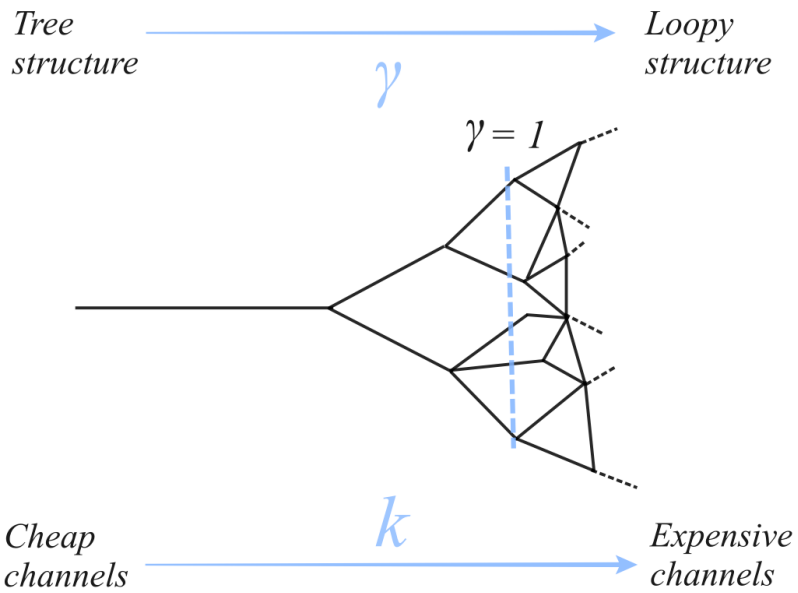

Figure 3.12: Bistable branching behaviour in a network featuring a transition between expensive and cheap channels with size

Chapter 4

Tree search toolkit

In last chapter we treated the optimization problem in an analytical way, trying to extend as far as possible the exact results we can get. We were finally able to characterize the main properties of model (3.12) minima. Despite the power of the framework we described, we still are left with a huge collection of local minima that, as for every optimization problem, we should compare 'by hand'. In particular when $0 < \gamma < 1$ each tree is a local optimum of our model (3.12). Note that the number of spanning trees on a 2D square cubic lattice grows exponentially with the number of nodes N. This means that from now on the quality of the description we are able to give, about the landscape of minima, depends on our numerical ability to explore this exponentially growing space of trees. In this section we are going to give a technical description of all the algorithm we used to face this task. The collection of all this methods represent the toolkit we built in order to explore the trees landscape, in the following chapter we will than see how the combination of this search methods is able to provide an overall picture of the optimal states properties.

4.1 EveryTree algorithm

After the description given in Chapter 3, It should be now clear that for every value of γ the local minima are always fulfilling the local optimal constraints (3.15) at each edge. At the same time, for sure, they have as well to fulfill the hydrodynamical fundamental requirements (3.9). Therefore, one idea to find a minimum is to start from a random initial configuration and iteratively impose, first the local optimality and then the hydrodynamical equations (Alg. 1). The fix point of this procedure will be a network for which both (3.15) and (3.9) holds, i.e. a local optimum.

Algorithm 1 EveryTree optimizer

procedure EVERYTREE(σ, κ)
    ▷ σ is the randomization strength
    ▷ κ is the initialization mean value for conductances
    $C_{init} \leftarrow$ Initialize the conductances matrix of the net ▷ every C_i is chosen randomly around the mean value κ with randomization strength σ
    while C not converged **do**
        impose local optimality on C
        impose hydrodynamical equations on C
    end while
    return C ▷ Optimized conductance matrix
end procedure

As starting states for the optimization procedure we used random generated grid networks as the one represented in Fig. 4.1.

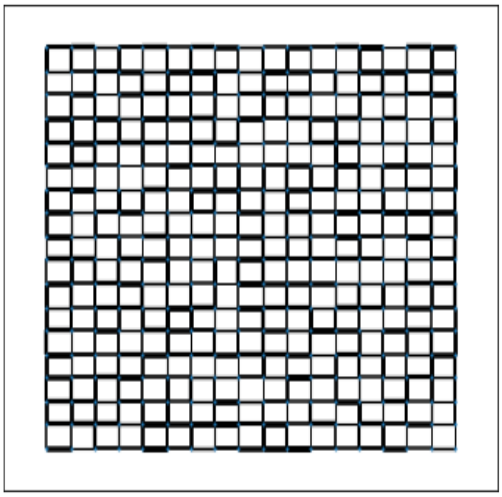

Figure 4.1: Random inizialized grid network (18x18 lattice)

In this initialization, weights (C_i) are picked, with an homogeneous probability distribution, in the interval $[\kappa - \Delta C, \kappa + \Delta C]$. We observed that the ratio between the radius of the interval and the mean value represent an important parameter, strongly linked to the qualitative shape of the final network. For this reason, we decided to define the randomization strength σ as:

$$\sigma = \frac{\Delta C}{\kappa}$$

note that $\sigma \in [0,1]$. With this algorithm we were successfully able to verify the phase transition occurring at $\gamma = 1$. Indeed, we observed a huge variety of local optimal trees for $\gamma < 1$ whereas, for $\gamma > 1$, the only solution was always the completely looped network (Fig. 4.2).

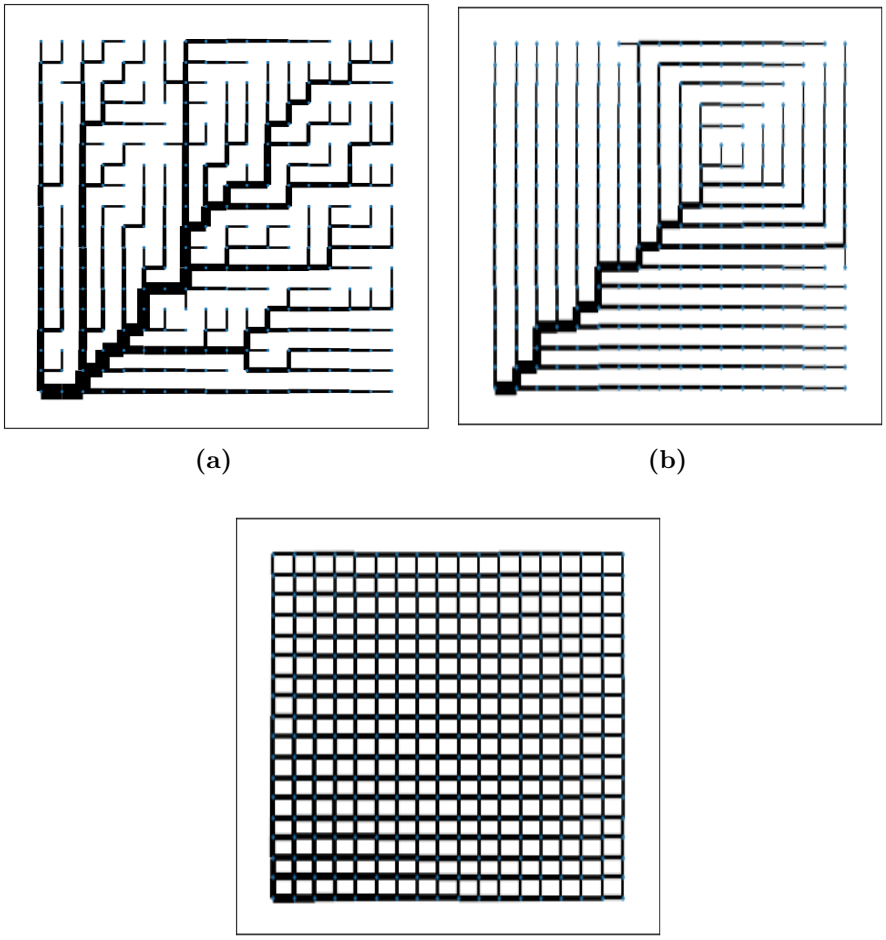

(a) **(b)**

(c)

Figure 4.2: Three local optimum found with EveryTree on a 18x18 lattice. (a) $\gamma = 0.5$, $\sigma = 1$ (b) $\gamma = 0.5$, $\sigma = 0$ (c) $\gamma = 2$, $\sigma = 1$

This algorithm update at every step all the conductances and stop on the first tree it finds. For this reason we call it 'EveryTree'. It is not the best in terms of performance (nor timing nor closeness to global optimum) but still, playing with his main parameter, i.e. the randomization strength σ, we are able to visit a wide set of topologies.

4.2 Greedy optimization

Since we know that the minima are all trees, we can even focus only on the space of networks without loops. We can then try to design a procedure in order to travel in the space of trees along trajectories on which the cost function is decreasing. Greedy algorithm does exactly that (Alg. 2).

Algorithm 2 Greedy optimizer

```
1: procedure GREEDY ALGORITHM(max_iter)
2:     ▷ max_iter is the maximum number of trial states that can be rejected
3:     Start from a random tree T
4:     compute his cost J(T)
5:     while iter < max_iter do
6:         produce a trial configuration T'
7:         if T' is loopless
8:             compute the cost of T'
9:             if J(T')<J(T)
10:                T ← T'                          ▷ accept T' as new state
11:            else
12:                iter += 1
13:    end while
14:    return T
15: end procedure
```

The idea is to start from an initial loop-less random configuration spanning the whole domain, evaluate its cost, and then to look for close trees that can provide a cost benefit. Of course this procedure depends on how we define the 'close trees' that we can propose as new trial configurations. In the greedy optimization algorithm we consider as neighbours accessible configurations all the trees that we can reach by randomly changing the position of a single edge. This procedure can't propose as future trial state a tree generated by a collective displacement of multiple edges and it is exactly from this strict rule for selecting the neighbours accessible states that arises its name. At each iteration, a random change in the configuration it is tried. If this change results in a loop-less configuration, the cost function J is computed. If the change reduces the numerical value of J, it is accepted; otherwise, the change is reversed. This process is repeated until the system is able to find a more favorable state in less that a given number of iterations max_{iter} (Fig. 4.3).

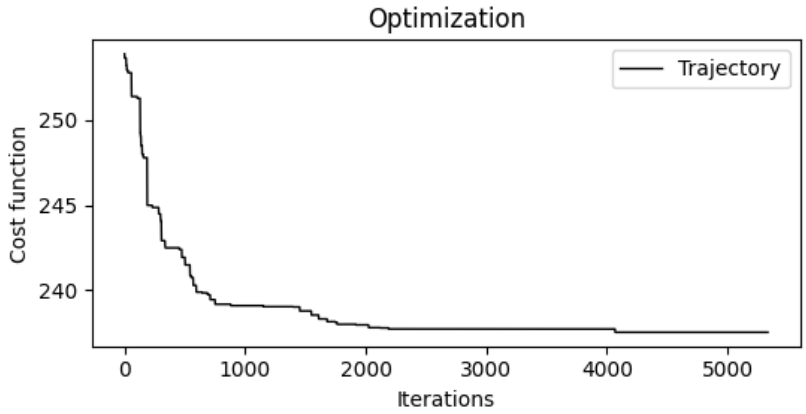

Figure 4.3: Example of cost trajectory produced using Greedy algorithm

The resulting network are often referred as *quasi-optimal* states because they are somehow optimal with respect of their neighborhood in the space of trees. The characteristics of those quasi-optimal trees however depends strongly on the choice of max_{iter}, as shown in Fig. 4.4. The Greedy algorithm, with its cautious approach, efficiently explores the space of loop-less tree configurations while seeking out optimal solutions.

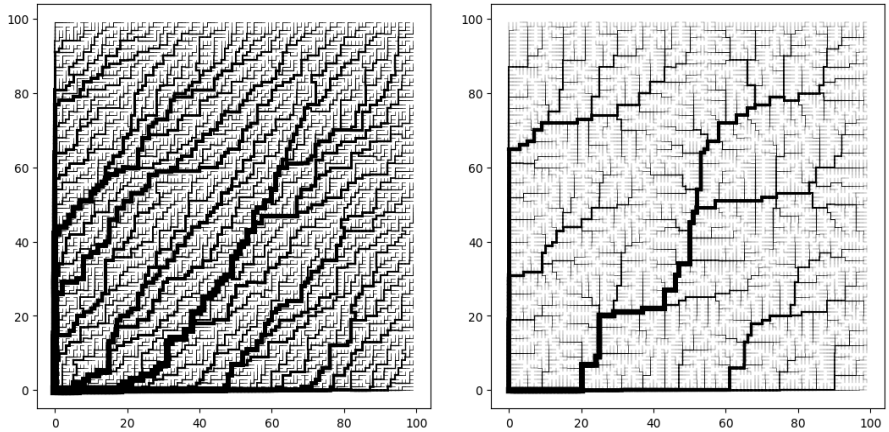

Figure 4.4: Two local optimum found with Greedy algorithm on a 100x100 lattice. (a) $\gamma = 0.5$, $max_{iter} = 100$ (b) $\gamma = 0.5$, $max_{iter} = 1000$

4.3 Metropolis algorithm

The Greedy algorithm is quite efficient but it is constrained to travel in the space of trees only following trajectories in which the cost decrease. This feature makes this algorithm unable to overcome even small cost barriers, potentially hiding more favorable region of the cost landscape. For this reason it is convenient to dispose of an algorithm that can either accept, with a given probability, some trial states that increase the cost J. We can do that by implementing the famous algorithm Metropolis (Alg. 3). It is just sufficient to slightly adjust the Greedy procedure (Alg. 2), the trial states are produced in the same way but now the acceptance rule is the following:

$$S_{t+1} = \begin{cases} S^{(T)} & e^{\frac{J(S_t)-J(S^{(T)})}{\tau}} > r \\ S_t & otherwise \end{cases} \tag{4.1}$$

Algorithm 3

```
1: procedure METROPOLIS(τ, max_iter)
2:     ▷ τ is the fictitious temperature
3:     ▷ max_iter is the maximum number of iterations that do not produce an
   overall improvement
4:     Start from a random tree T
5:     Compute his cost J(T)
6:     J_best ← J(T)
7:     while iter < max_iter do
8:         produce a trial configuration T'
9:         if T' is loopless
10:            compute the cost of T'
11:            sample r ∈ [0,1] from the uniform distribution
12:            if e^((J(T)−J(T'))/τ) > r
13:                T ← T'                          ▷ accept T' as new state
14:                if J(T) < J_best
15:                    J_best ← J(T)
16:                else
17:                    iter += 1
18:    end while
19:    return T
20: end procedure
```

where S_t is the network obtained at the *t-th* iteration of the algorithm, $S^{(T)}$ is the trial state proposed, τ is a fictitious temperature and r in a number uniformly sampled between 0 and 1. The fictitious temperature is a parameter that symbolize the amount of 'energy' present in the system. For $\tau \to \infty$ every trial state can be accepted whereas for $\tau \to 0$ the algorithm accept only states that decrease the cost (reducing to the Greedy strategy). For this reason the performance of Metropolis algorithm strictly depends on our choice of τ. As shown in Fig. 4.5 if the temperature is sufficiently low the system decrease his cost and then stabilize its behaviour on an average value with some noise. Instead if the temperature is too high the cost rapidly change exploiting the big thermal fluctuations and in general goes towards values even bigger than the random initial condition.

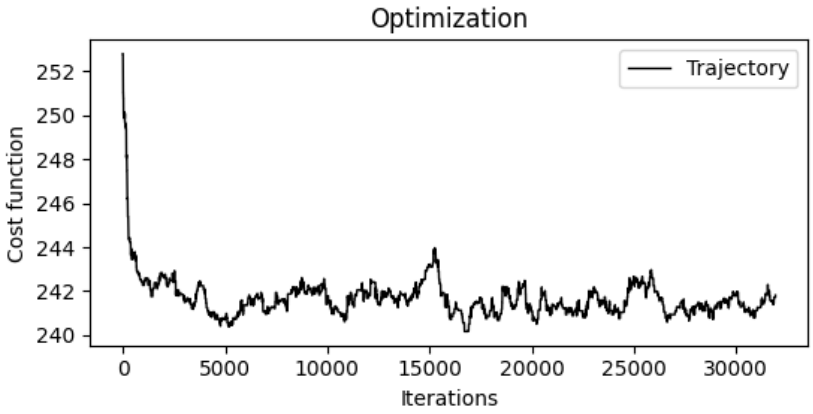

(a)

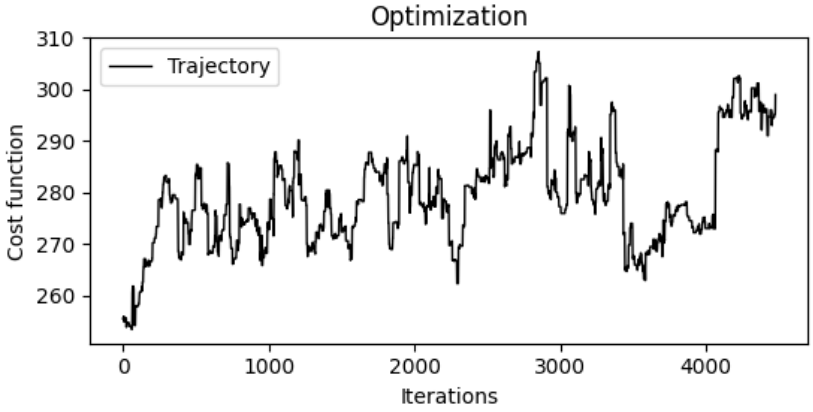

(b)

Figure 4.5: Two cost trajectories generated with Metropolis algorithm (a) $\tau = 0.1$ (b) $\tau = 10$

4.4 Simulated annealing

In order to fully exploit the possibility of overcoming cost barriers, introduced with Metropolis algorithm , we can further act on the fictitious temperature. In fact if we do not keep τ fixed we can better employ the power of the 'thermal energy' for our ends. This is precisely the idea behind the famous optimization strategy called Simulated Annealing [41]. Thus, we can do the following, we use algorithm Metropolis starting from an high temperature, then after a given number of iterations n_{iter} we lower τ. This scheme is repeated for a given number of times n_{batch} until we reach a sufficiently low temperature. However this procedure is far more complex than it can seems. In particular the quality of the result depends strongly on how do we decrease the temperature. The scheme we use to perform the annealing, i.e. the choice of the initial themperature, n_{batch},n_{iter} and other parameters, is commonly called cooling schedule. We based the selection of the initial temperature on the work of Ben-Ameur [42]. The idea is essentially just to compute the ratio f between proposed and accepted states and to increase the temperature until we reach $f \approx 0.8$. Instead for performing the cooling we followed the path presented by Atiqullah [43] where the temperature is lowered as shown in Fig. 4.7. In this cooling schedule we can distinguish between three separate phases (Fig. 4.6). At first, we allow for large energy fluctuations, in order to explore freely the tree space. Then, we start our landing towards a local region, and in this phase we still are able to accept trial states that increase the cost. Finally, we perform a fine tuning in the niche of the cost landscape we ended up in.

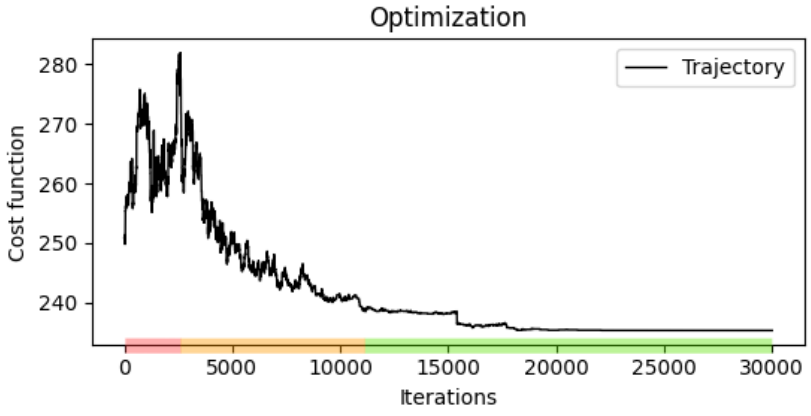

Figure 4.6: Example of cost trajectory produced using Simulated Annealing. Is easy to see the separation between the three main phases: free exploration (red), descent toward a local region (orange) and fine tuning (green)

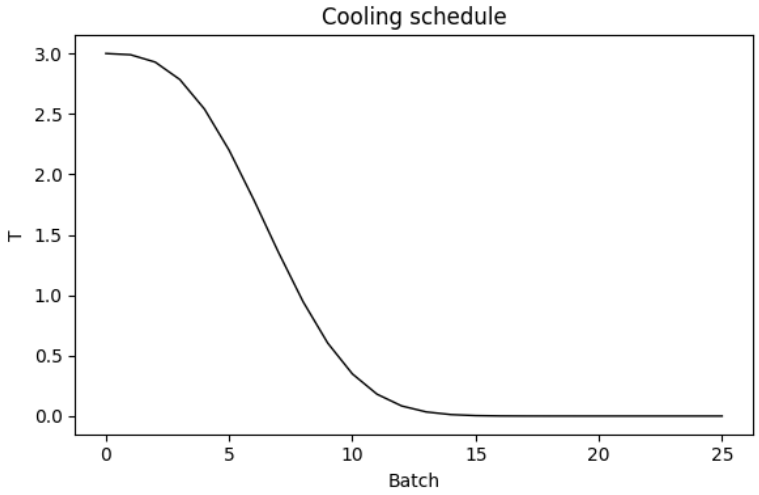

Figure 4.7: Cooling schedule designed following Atiqullah's proposal [43]

Algorithm 4

procedure SIMULATED ANNEALING($\bar{CS}$)
    ▷ $\bar{CS}$ is the vector of parameters needed to implement the cooling schedule, in the simplest case we can consider as example: $\bar{CS} = T_I, T_F, n_{batch}, n_{iter}$
    Start from a random tree T
    Compute his cost J(T)
    $J_{best} \leftarrow J(T)$
    for $t \in 1 : n_{batch}$ **do**
        while $iter < n_{iter}$ **do**
            produce a trial configuration T'
            if T' is loopless
                $iter$ += 1
                compute the cost of T'
                sample $r \in [0,1]$ from the uniform distribution
                if $e^{\frac{J(T)-J(T')}{\tau}} > r$
                    $T \leftarrow T'$ ▷ accept T' as new state
                    if $J(T) < J_{best}$
                        $J_{best} \leftarrow J(T)$
        end while
        $\tau = \tau - \frac{T_I - T_F}{n_{batch}}$
    end for
    return T
end procedure

Chapter 5

The present knowledge of the minima landscape

After having presented various search methods in Chapter 4, we are now ready to explore the domain of (local) optimal networks. Exploiting the code we developed, we successfully reproduced all the behaviors documented in literature. In this chapter, our goal is to present a comprehensive overview of the present understanding of the minima landscape. We aim to devise an effective representation that consolidates the key understandings gathered by previous researchers and, additionally, we will try to augment our comprehension by introducing novel details. In particular, we will provide a characterization of an interesting behavior occurring at the ground state.

5.1 Different degrees of optimality

In order to give an effective idea of the possible characteristics that different nets are able to exhibit it is fundamental to find a good set of parameters that can well capture the separation between specific behaviours. In fact the original space of networks, described in section 3.1, is an incredibly high dimensional space that is impossible to take into account directly. The true challenge is instead to find the mentioned set of parameters that naturally separate networks families in a low dimensional space, providing a more intuitive picture. The first parameter that we will consider is γ. In fact γ is well known to be responsible for the transition between a completely loopy network and tree structures (Fig. 5.1).

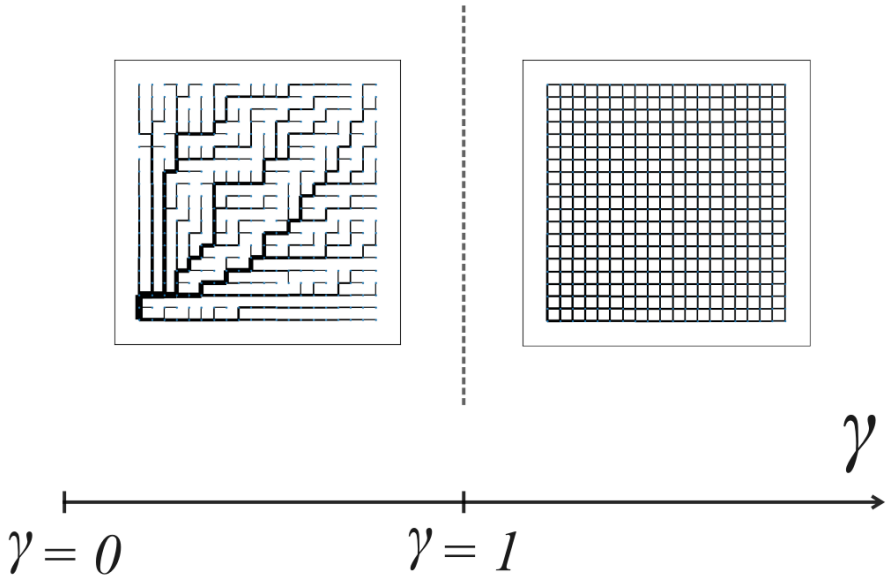

Figure 5.1: The role of γ here illustrated in a schematic.

This property arise from the application of the local optimality principle and it is analytically described through the famous Banavar's proof, as discussed in Chapter 4. For $\gamma > 1$ the topology that minimize the cost is unique. The specific characteristics of the channels can still vary but maintaining the completely looped arrangement. For $\gamma < 1$ instead all the trees are local minima. Despite that, we have to consider that by modifying γ and other parameters as well, the relation existing between this different minima can change. Now we will focus on the case $0 < \gamma < 1$ that is the most interesting one. We are interesting in introducing a parameter that accounts for different degrees of optimality of the system. Of course the cost function J previously described appears to be a perfect candidate for that role. But here we decided to use instead another variable that can more effectively cover the same meaning. In order to present our choice we have to introduce first the thermodynamical interpretation of channel networks.

5.1.1 Thermodynamics of channel networks

It proves advantageous to draw an analogy with classical thermodynamics, as undertaken by Rinaldo and Troutman [44] [45]. This connection offers an effective means to discern essential features within certain families of minima. However, it is crucial to be cautious in considering this link, given the absence of a rigorous

physical microscopic description of the system. Therefore, this analogy serves as purely illustrative purpose and all the phenomenological conclusion that we can draw are rather speculative. Let's call S the set of all the spanning trees rooted in the lower left corner (as in our setup). For every tree $s \in S$ we can thus define a Boltzmann-like probability:

$$P(s) \propto e^{\frac{-J(s)}{\tau}} \tag{5.1}$$

where τ is a fictitious temperature that mimic the role of the real temperature T for classic thermodynamic systems. At this point, if we call $N(J_i)$ the number of spanning trees that share exactly the same cost (energy in the thermodynamic language) J_i, we can also define the probability of a configuration with energy J_i:

$$\begin{aligned} P(s \,|\, J(s) = J_i) &\propto N(J_i)\, e^{\frac{-J_i}{\tau}} \\ &\propto e^{\frac{-(J_i - \tau\, lnN(J_i))}{\tau}} \\ &\propto e^{\frac{-F(J_i)}{\tau}} \end{aligned} \tag{5.2}$$

where we have defined, in analogy with the classic statistical mechanics formulation, an entropy $S(J) = lnN(J)$ and a free energy $F(J) = J - \tau\, S(J)$. Note that we are just employing the thermodynamic analogy in order to better capture different network properties. This description is able to artificially introduce the effect of entropy and imperfect search in our formulation. This is fundamental in order to reproduce the same phenomenology observed in nature. A wide range of behaviours can be reproduced changing τ and exploring the spanning tree space with the toolkit of simulation algorithm described in Chapter 4. Later on we will explore the consequences of fully exploiting this thermodynamic framework. But, before going in detail into that, there is still another important concept that we must define: the notion of contributing area.

5.1.2 The contributing area

The contributing area is a quantity holding a profound meaning that has been widely studied specifically in the domain of river drainage networks [46] [47] [48]. However, its relevance is transversal since it represents an aggregate measure able to well capture some overall characteristics of a general channel network. In the discrete case, the one we are considering, the contributing area can be defined at each node as:

$$a_i = \sum_{j \in N_i} a_j W_{ji} + s_i \tag{5.3}$$

where N_i is the neighbours set of node i, s_i is the load demand at i-*th* node and W_{ji} is equal to 1 if the flux is directed from j towards i and it is instead null

otherwise. Thus intuitively a_i, for us, is just the total flow entering (or exiting) the *i-th* node. Now, it should be considered that there exist several empirical laws such as the famous results of Horton [49] and Hack [50] that pointed out the existence of scaling relations in natural networks [51]. Moreover, several experimental findings have in particular outlined a scaling behaviour for the contributing area in natural river networks across several scales (as shown in Fig. 5.2 [39]).

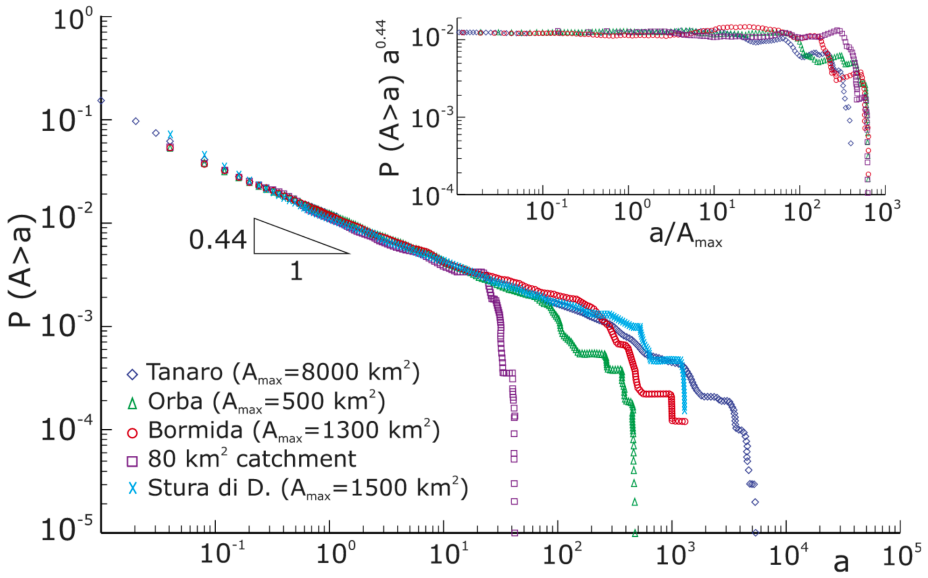

Figure 5.2: Statistical evidence of the cumulative contributing area $P(A > a)$ scaling behavior studied by Rinaldo et al. [39]

Interestingly in the 90' some studies showed that the empirical laws and the practical evidence could be all related together and explained by proposing a *finite scaling ansatz* for the contributing area distribution [52] [53] [45] [17]. The latter can be stated as follow:

$$P(a) = a^{-t} f(\frac{a}{A_C}) \tag{5.4}$$

here, $f(x)$ represent a scaling function that incorporate finite size effects, while A_C denote the characteristic area of the system. Note that $f(x)$ is assumed to exhibit the following properties: as x approaches infinity, f go to zero sufficiently fast to ensure normalization; when x tends to zero, f approach a constant, yielding a power law. Moreover this scaling behaviour has been widely observed also in the numerical outcomes of OCNs models (Fig. 5.3).

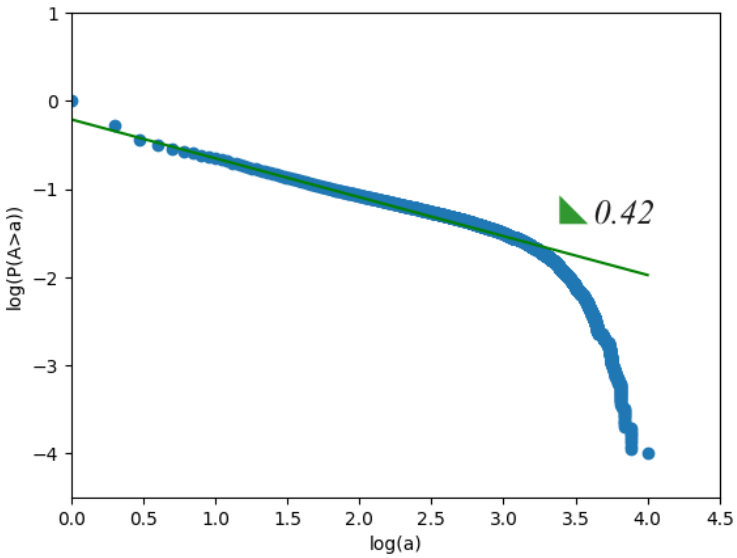

Figure 5.3: Our results showing the existence of scaling for $P(A > a)$ in the OCN model. The graph show the ensemble average of 100 networks, with size 100x100, produced with the greedy algorithm for $(\alpha = 1, \gamma = 0.5)$. Note that the scaling exponent $\beta = 0.42$ is the one found in average also in natural networks.

The latter provided a promising sign that the OCN formulation, relying on its energy minimization principles, is indeed able to well capture the behaviour of natural networks. Notably if we consider together the idea of energy minimization and scaling ansatz we are able [52] to find the scaling exponents that theoretically assure the minimum energy (cost). This is the best analytical result we can dispose nowadays about the features of the absolute minimum. In particular the latter told us that the optimum solution should feature a scaling of the cumulative contributing area $P(A > a)$ with an exponent β equal to 0.5 [54].

5.1.3 The role of τ

Now, we can go back to the issue of finding the right parameters to construct a meaningful phase diagram. We have already discussed the significance behind the choice of γ and explained why it provides fundamental information. The next parameter we are going to consider is τ, the fictitious temperature introduced within the thermodynamic analogy in section 5.1. This parameter enables us to distinguish between classes of very interesting behaviors. All the key results are summarized in Fig. 5.4. Let's closely examine it.

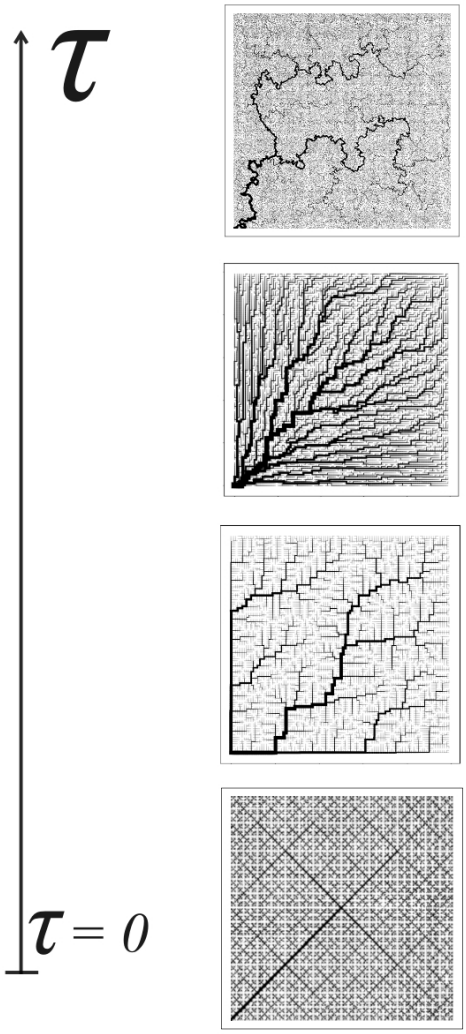

Figure 5.4: The role of τ here illustrated in a schematic.

Beginning with high values of τ, we can comprehend the properties of an ensemble of networks generated by maximizing entropy. In this 'high temperature' regime it is the degeneration $N(J_i)$ that dominates over the energy (cost) J_i. The interesting feature of those network is that they are clearly fractals. Even at eyesight their self-similar geometry is evident. Note that one can produce those networks using the Metropolis algorithm (Chapter 4) by choosing a sufficiently high value for τ and evolving the network for a high number of iterations. Let's go on and examine what happens if we lower τ. The striking fractal behaviour goes

away and we start seeing quite inefficient trees that do not show any particular interesting property. They are just expensive valid solution of the channel problem that can typically be produced using the EveryTree algorithm described in Chapter 4. Then if we continue to lower τ an interesting behaviour emerge. The trees start developing again self similarity on a growing number of scales. We can capture this self similar behaviour through the scaling law of the cumulative contributing area. Here it is fundamental to note that if we either use the Greedy algorithm or the Metropolis one, with a low τ, (Chapter 4) we produce network ensembles that match very well with experimental data of natural networks. Specifically, they match the scaling exponent $\beta \approx 0.42$ found commonly in rivers. On the other hand, if we push the minimization to the edge of our capabilities, using Simulated Annealing (Chapter 4), we approach the scaling exponent $\beta = 0.5$. Finally, the last bottom picture in Fig. 5.4, display a Peano's fractal. This space filling geometry is one of those described by Giuseppe Peano, originally from Turin, at the end of the 19'th century. Since it features exactly the scaling exponent $\beta = 0.5$ it is commonly taken as an upper bond for the ground state energy. The recursive construction procedure of the Peano fractal is dysplaied in Fig. 5.6.

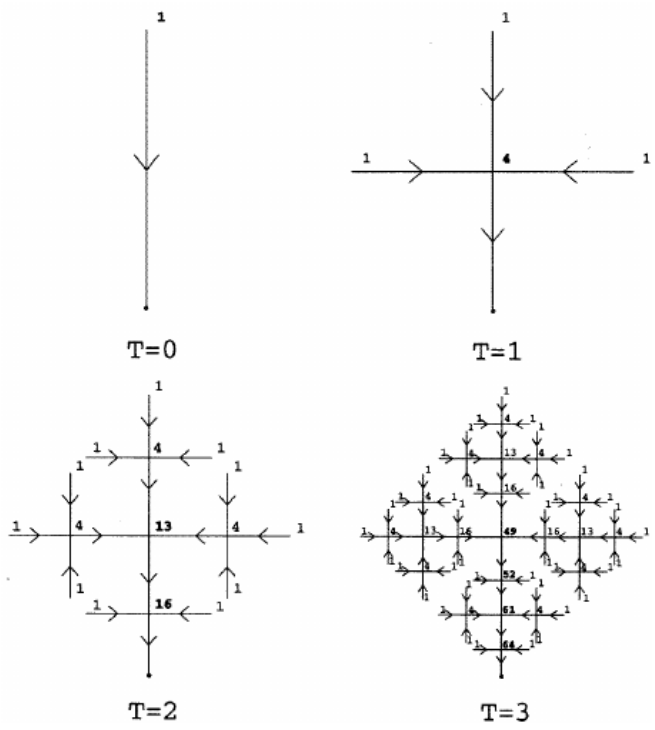

Figure 5.5: Construction of the Peano fractal [55], T represent the iterations of the procedure whereas the numbers written near each node correspond to their contributing areas.

At the bottom line τ seems to us a good parameter to describe networks properties for two main reasons. Firstly, because we are able to better visualize some asymptotic behaviours. For example taking $\tau = 0$ we can always directly refer to the proprieties of the global minimum whereas, instead, the exact cost J of the absolute optimum would change in different conditions and is not generally even known. This allow us to represent in a easier way the ground state of the model. In the opposite limit, taking $\tau \to \infty$ we can instead visualize the entropy dominated networks that are more interesting than the structures simply maximizing J. On the other hand, by using τ we are able to more effectively describe real world scenarios in which the appearance of a structure is both related to its cost and its probability. In next section we are going to examine more carefully the ground state.

5.2 The ground state

The ground state represent the absolute minimum (or minima) of the cost function, corresponding to the limit $\tau = 0$ in the thermodynamic interpretation. Its properties can vary while changing the parameters of the model and they are clearly of great interest. Despite that, there is still a lot of mystery beside its exact features. The best analytical result is provided under the scaling hypothesis discussed in section 5.1.2. The latter suggest that the absolute optimum is reached when the scaling exponent β of the cumulative contributing area $P(A > a)$ is exactly equal to 0.5 as for the Peano fractal basin. However, as we discussed, the Peano geometry represent only a theoretical upper bond to the real solution, since it is obtained in the contest of the scaling ansatz. More in general, if we want to go beyond that, our only possibility is to recur to numerical results.

5.2.1 The fish bone network

What we noticed is that it is possible to deepen our knowledge of the ground state (GS) by studying how it changes with the number of nodes N. But, in contrast with previous results, we found that there is a region of the GS phase diagram were the absolute optimum seems to be a specific geometry that do not exhibit scaling. The latter is the topology we called 'fish bone network' (Fig. 5.6). One can think that this limit is reached when the dimension of the domain do not allow for scaling to appear because the influence of the geometrical boundary conditions is too strong. It should although be stressed once more that this result isn't analytical but it arises as the outcome of an intense set of numerical observations.

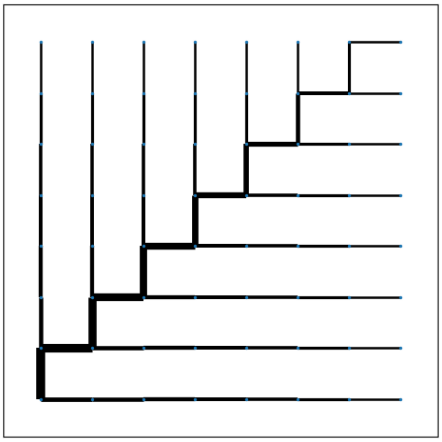

Figure 5.6: The fish bone network

Additionally, we noticed that the complete breaking of scaling and the emergence of the fish bone network, as the best candidate for the GS, depends not only on the size N of the system, but also on the γ exponent. We were therefore able to draw a transition line that mark this shift on the GS behaviour across the (L, γ) plane (Fig. 5.7). Where L is the number of nodes on an edge, specifically $N = L^2$.

.

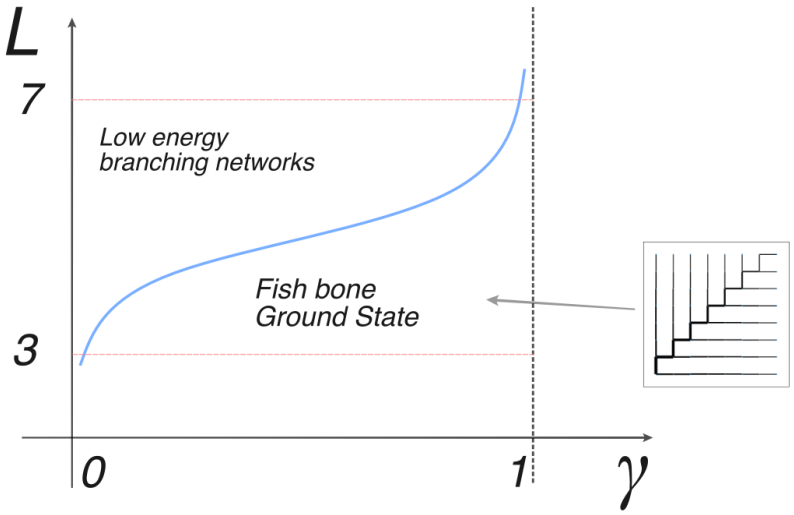

Figure 5.7: The (L, γ) Ground state diagram

Note that, as we stay below the blue line in Fig. 5.7, we consistently end always

on the same minima, the fish bone network, by using all the methods in our toolkit (Chapter 4). On the other hand, if we cross that boundary either by enlarging the size of the domain or by lowering γ, the numerical methods start to produce a variety of different solutions at each run and it is impossible to outline a global minimum geometry. As last comment, let's just point out that, even if for bigger networks the fish bone geometry is not a good candidate as global minimum (in fact it gets in general very expensive), still, we can recognize something similar at the lower scales. To understand this qualitative remark let's look at Fig. 5.8.

.

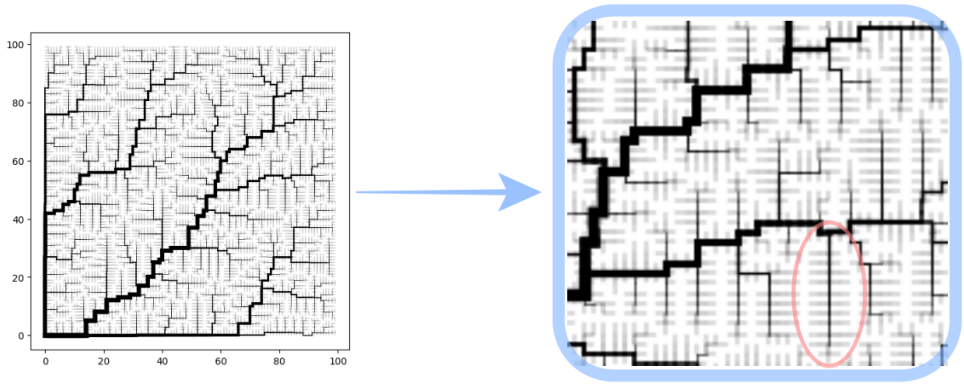

Figure 5.8: Zoom in a network of size 100x100 obtained with simulated annealing for $\gamma = 0.5$

In fact, we can think that each time a subbranch is created during a bifurcation, the optimal solution for that subbranch could be computed as a variation of the original problem, but with a reduced number of nodes and a more irregular domain shape. Consequently, as the branching scale approaches the limit where the fish bone topology represents the absolute minimum, one might expect it to emerges. However, what is observed at the lower scales, in our low cost networks, is not precisely the fish bone structure, but rather an 'antenna-like' arrangement, highlighted in red in Figure 5.8. Although sharing similarities with the fish bone pattern, it is distinct. This observation could imply that the fish bone solution might be superior but is highly improbable to be observed with the current algorithms. Alternatively, it can suggest that the system tends to adopt different boundary conditions for organizing smaller subbranches compared to our usual setup, i.e., a square domain with a single inlet placed in a corner.

5.2.2 The whole picture

Finally, we can consider all together in order to provide the comprehensive picture we promised at the beginning of this section. All the behaviours we discussed can be regrouped in the (γ, τ, N) phase diagram displayed in Fig. 5.9.

.

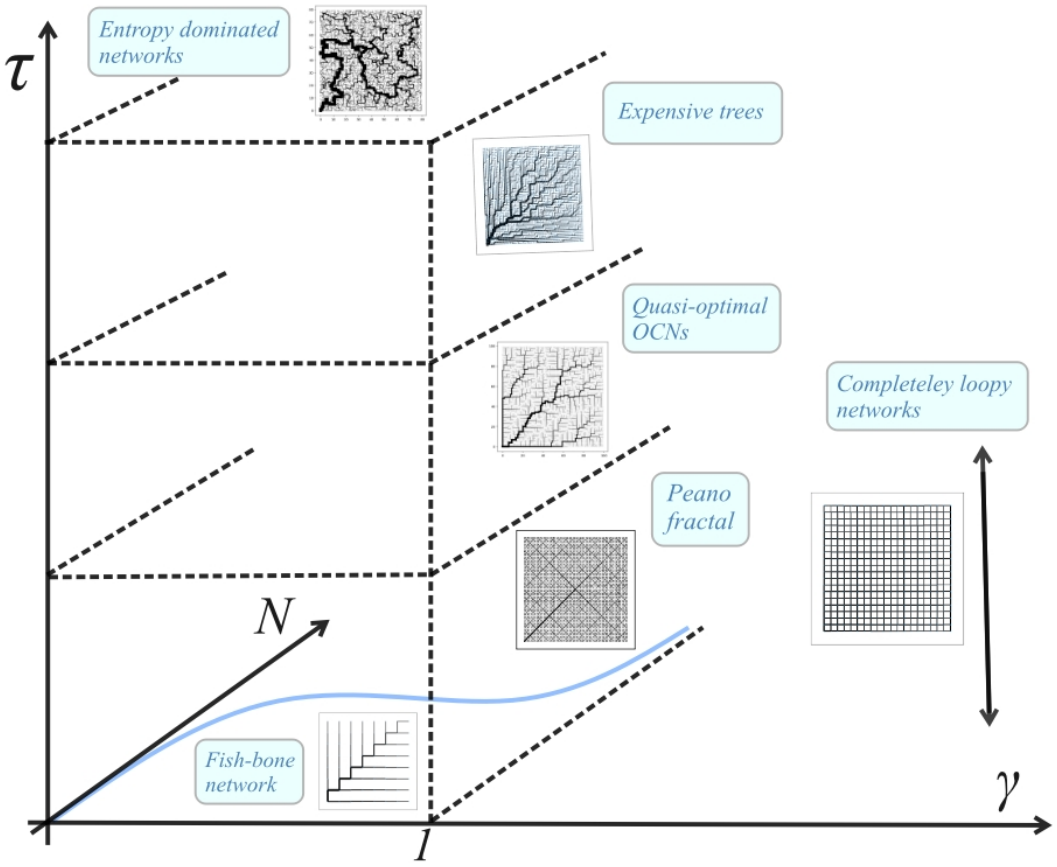

Figure 5.9: The (γ, τ, N) phase diagram

It is important to underline that this representation is able to show us, in a concise schematic, all we know about OCNs phenomenology. However, it is evident that our knowledge is not exhaustive. The families of networks we have managed to characterize delineate certain key behaviors within the exponentially expanding space of trees. Yet, it is reasonable to presume that there are still other meaningful clusters of networks awaiting identification and careful investigation. Furthermore it would be important to comprehend the mechanisms governing the transition between different groups of networks. For the moment it is qualitatively clear

that changing τ act on the number of scales on which self similarity is observed. Either originating the typical self similar behaviour exhibited by *entropy dominated networks* or instead the one of *quasi-optimal OCNs*. But for example the behaviour at the proximity of the blue line in Fig. 5.9, representing the transition line under which the *fish bone network* is the global optimum, is poorly understood. Moreover we should recall that, our analysis operates within the assumption of a 2D square lattice geometry, featuring a unique inlet located in the lower left corner. Preliminary investigations suggest a non-trivial shift in the scenario when the domain's shape, lattice geometry, or the number and positions of inlets are changed. The symmetry of the system appears to yield significant influence, yet this, too, remains a subject for future exploration.

Chapter 6

Conclusions

The study of Optimal Channel Networks represent a fertile domain that has already been extensively explored from diverse perspectives. However, still today there are numerous open questions and new avenues to be explored. We examined the path that brought to the contemporary knowledge of OCNs, reviewing the most significant stages. During this journey we gathered different ideas and results coming from a wide range of perspectives. From the local approach of Hess and Murray to the more modern inquiry for the overall topological features of networks. From the natural river inspired perspective of Rodriguez-Iturbe and Rinaldo to the biological network studies of Bohn and Corson. From the analytical results of Banavar to the thermodynamical approach of Maritan. We gathered the key findings of more than a century of research making benefits of many intuitions crafted with different approaches and aims. In the end, we tried to draw an overall picture, with the goal to show that, the mentioned studies, could be well summarized in a unified discussion. Moreover, in delineating this comprehensive picture, we were able to extend further the generalization, allowing to gave birth to new results and to provide an original contribution.

At the bottom line our research can be summarized in three fundamental points: the derivation of a unified model for OCNs, the description of a systematic optimization framework and the proposal of a phase diagram that try to capture the contemporary understanding of channel networks. For what concern the first issue, we proposed a new model for the networks cost function that well reproduce many previous separate findings. Furthermore, our model seems to be the first able to fully account for some other flow processes. Specifically, it can be used to define the OCN problem in the whole laminar-turbulent transition. This detail is interesting since it allows to account for networks featuring a dynamical transitioning behaviour. We showed how this aspect is able to explain the emergence of hierarchical loopy branching either at the low scales or at the big ones. In particular, the latter could provide a new tool for explaining the well documented appearance of loops at the

low scales of natural channel networks. It is worth to stress that this would be a good result since it is the first time that a hierarchical structure featuring loops can be explained in the context of stationary regimes.

Our second effort was to establish a clear description of the optimization framework. In particular, we underlined how the optimization process should pass through two fundamental principles: the principles of local and global optimality. While the second is indispensable and should be considered as the basis of any OCN model, we tried to argue that the first one is actually unnecessary. We gave an exact proof for a simple case and we developed some arguments for the general situation. Nevertheless, a decisive demonstration remain the goal of future research.

Finally, we developed a solid toolkit of numerical algorithms in order to map the networks space and try to understand it. Our aim was the one of identifying a minimum set of essential parameters able to well capture all the network phenomenology present in the literature. We then proposed a (τ, γ, L) phase diagram, showing that it can be used to summarize the current knowledge and to introduce a new curious effect as well. In fact, by making use of the latter representation, we observed a transition happening in the phase space: the global optimum is well-defined for sufficiently small networks, coinciding with the structure we referred to as the 'fish bone network'. This result seems to represents the first numerically achieved global optimum and it is also of significant interest for gaining further insights into the smallest scale of larger networks.

We hope that with this thesis, we were able to contribute valuable ideas to the understanding of Optimal Channel Networks (OCNs) and foster further exploration in this research field. We achieved a few new results, which we aim to publish in a journal paper, and we have uncovered many intriguing avenues of research that we are eager to explore. Despite its longstanding roots, the optimal channel networks problem continues to offer ample opportunities for further investigation.

Appendix A

The two resistor loop

In this appendix we will consider the complete analytical solution for the simplest possible network we can think of: the two resistor loop. The latter, can be represented as shown in Fig. A.1. Therefore, we have only two node and the loads requirements are just $(s_1 = x, s_2 = -x)$.

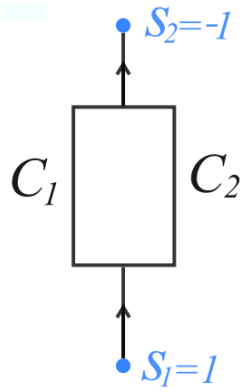

Figure A.1: The two resistor loop

Given that we are dealing with only two edges, we can try to graphically represent the cost landscape. The problem is that it is not intuitive to guess how does $J(C_1, C_2)$ behave for every combination of C_1 and C_2. Despite that, for sure we know, in analogy with our very definition of cost (see section 3.2), how $J(C_1, C_2)$ should look like when either C_1 or C_2 are equal to zero. We expect that on this case, showed in Fig. A.2, we are completely able to solve the minimization problem just by imposing stationarity in terms of the conductances. The reason why we can do that is because the flow distribution is fixed, since all the entering current is forced to pass across the only non null conductance.

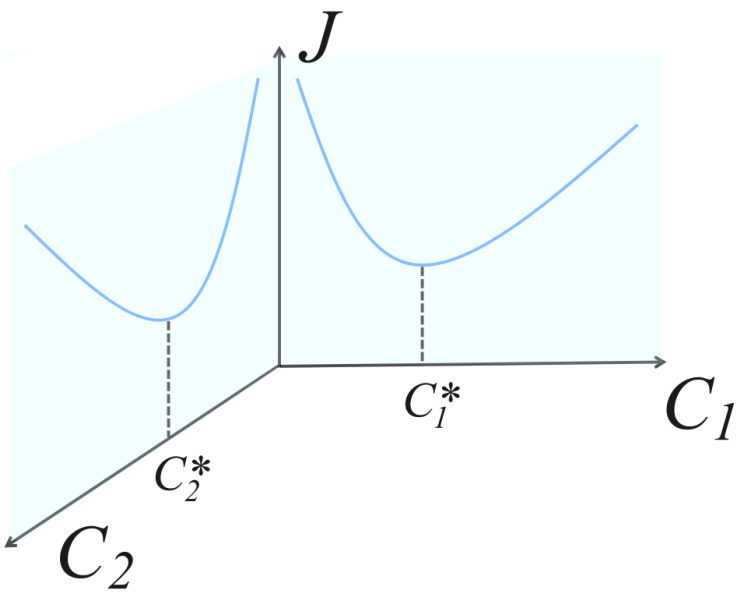

Figure A.2: 3D representation of $J(C_1, C_2)$. In the picture the cost is displayed only on the planes for which either C_1 or C_2 are equal to zero.

As mentioned in section 3.2, the minimization is complicated in general by the fact that as we change the values for C_1 and C_2 also the currents flowing in the two channels change, by affecting the total cost.

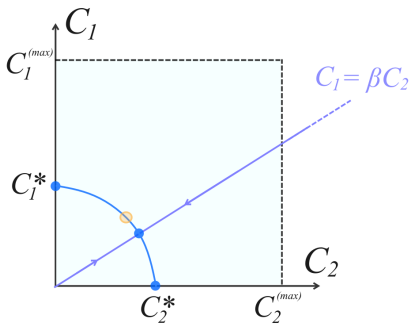

Figure A.3: Representation of Ω, the space of all possible networks, in this simple case. Note that we also considered some boundary values for the conductances.

An idea to overcome this problem if to exploit the following trick. Note that, if we change the values for C_1 and C_2 while keeping their ratio (β) equal to a constant, the flow distribution do not change and thus we are able to solve exactly the optimization problem (Fig. A.3). Therefore hopefully we can solve the problem

for a generic ratio and then mature an overall understanding on the cost functional behavior. The latter can be done by using the Lagrange multiplier method and considering the constraint of constant ratio. Graphically it amounts on solving the original problem but with the additional constrain to remain on the violet line (Fig.A.3) of the domain. We can thus write:

$$L(C_1, C_2, \mu)^{(\beta)} = \sum_{i=1,2} Q_i^{\frac{\alpha+1}{\alpha}} C_i^{\frac{-1}{\alpha}} + bC_i^{\gamma} + \mu(\frac{C_2}{C_1} - \beta)$$

$$\begin{cases} \frac{\partial L}{\partial C_1} = (\frac{-1}{\alpha}) C_1^{-\frac{1}{\alpha}-1} Q_1^{\frac{\alpha+1}{\alpha}} + b\gamma C_1^{\gamma-1} - \mu\frac{C_1}{C_2^2} = 0 \\ \frac{\partial L}{\partial C_2} = (-\frac{1}{\alpha}) C_2^{\frac{-1}{\alpha}-1} Q_2^{\frac{\alpha+1}{\alpha}} + b\gamma C_2^{\gamma-1} + \frac{\mu}{C_1} = 0 \end{cases}$$

$$\begin{cases} Q_1^{\frac{\alpha+1}{\alpha}} = \alpha b\gamma C_1^{\gamma+\frac{1}{\alpha}} - \mu\alpha C_2 C_1^{\frac{1}{\alpha}-1} \\ Q_2^{\frac{\alpha+1}{\alpha}} = \alpha b\gamma C_2^{\gamma+\frac{1}{\alpha}} + \mu\alpha\frac{C_2^{\frac{1}{\alpha}+1}}{C_1} \end{cases} \tag{A.1}$$

$$\beta^{\frac{\alpha+1}{\alpha}} = \frac{b\gamma C_2^{\gamma+\frac{1}{\alpha}} + \mu\frac{C_2}{C_1} C_2^{\frac{1}{\alpha}}}{b\gamma C_1^{\gamma+\frac{1}{\alpha}} - \mu\frac{C_2}{C_1} C_1^{\frac{1}{\alpha}}}$$

$$\begin{cases} C_1^* = \left[\frac{\mu(\beta^{\frac{2\alpha+1}{\alpha}} + \beta^{\frac{\alpha+1}{\alpha}})}{b\gamma(\beta^{\frac{\alpha+1}{\alpha}} - \beta^{\frac{\alpha\gamma+1}{\alpha}})}\right]^{\frac{1}{\gamma}} \\ C_2^* = \beta C_1^* \end{cases}$$

where we defined a Lagrangian and we considered his stationarity both with respect to C_1 and C_2. Interestingly, it can be easily shown that $C_1/C_2 = \beta \implies Q_1/Q_2 = \beta$. We can find the exact value for the Lagrange multiplier μ by substituting C_1^* and C_2^* in the stationarity conditions. Furthermore, it is easy to verify that, for our constant ratio scenario, the currents are exactly:

$$\begin{cases} Q_1 = \frac{1}{1+\beta} \\ Q_2 = \frac{\beta}{1+\beta} \end{cases} \tag{A.2}$$

By substituting those information we finally get the optimal values for the

conductances as a function of their ratio:

$$\begin{cases} C_1^* = \left(\frac{1}{\beta\alpha\gamma}\frac{1+\beta}{1+\beta^\gamma}\right)^{\frac{\alpha}{\alpha\gamma+1}} Q_1^{\frac{\alpha+1}{\alpha\gamma+1}} \\ C_2^* = \left(\frac{\beta^{\alpha(\gamma+1)}}{\beta\alpha\gamma}\frac{1+\beta}{1+\beta^\gamma}\right)^{\frac{\alpha}{\alpha\gamma+1}} Q_2^{\frac{\alpha+1}{\alpha\gamma+1}} \end{cases} \tag{A.3}$$

Equation (A.3) is a generalization of the stationarity condition (3.17) that now holds for every particular value of β. Thus, since by changing β we are able to span all the domain Ω, we can now rigorously reduce the candidate minima to all the points fulfilling (A.3). Note that in this case the application of the principle of local optimality would reduce the points to take into account to only three configuration: the configuration (C_1^*,0), $(0, C_2^*)$ and the symmetrical one. Those are exactly the cases in which (A.3) and (3.17) match, respectively related to $\beta = 0{,}1, \infty$. But now we are able to express exactly a whole line of stationary points as shown in Fig. A.3. Therefore, the last thing that we have to do to completely solve our problem is to consider what happens on this line. We can do that in two steps. The first is to rewrite the cost by using (A.3) in order to consider only the points on the stationary line. In doing that we will be able to finally write $J(C_1^*, C_2^*)$ as a function of the ratio β alone. Subsequently, the second step will be to consider the derivative of $J(\beta)$ in terms of β, to completely understand its behaviour all over the domain Ω. Let's start by substituting (A.3) in our model (remember that $C_2 = \beta C_1$ and $\Gamma = \gamma(\alpha+1)/(\alpha\gamma+1)$):

$$\begin{aligned} J(C_1, C_2) &= \sum_{i=1,2} Q_i^{\frac{\alpha+1}{\alpha}} C_i^{\frac{-1}{\alpha}} + bC_i^\gamma \\ J(C_1^*, C_2^*) &= (1+\beta)\left(\frac{1}{\beta\alpha\gamma}\frac{1+\beta}{1+\beta^\gamma}\right)^{-\frac{1}{\alpha\gamma+1}} Q_1^\Gamma + b(1+\beta^\gamma)\left(\frac{1}{\beta\alpha\gamma}\frac{1+\beta}{1+\beta^\gamma}\right)^{\frac{\alpha\gamma}{\alpha\gamma+1}} Q_1^\Gamma \\ &= Q_1^\Gamma\left[(1+\beta)\left(\frac{1}{\beta\alpha\gamma}\frac{1+\beta}{1+\beta^\gamma}\right)^{-\frac{1}{\alpha\gamma+1}} + b(1+\beta^\gamma)\left(\frac{1}{\beta\alpha\gamma}\frac{1+\beta}{1+\beta^\gamma}\right)^{\frac{\alpha\gamma}{\alpha\gamma+1}}\right] \\ &= \left(\frac{1}{b\alpha\gamma}\right)^{-\frac{1}{\alpha\gamma+1}} \frac{(1+\beta)^{1-\frac{1}{\alpha\gamma+1}-\Gamma}}{(1+\beta^\gamma)^{-\frac{1}{\alpha\gamma+1}}} + b\left(\frac{1}{b\alpha\gamma}\right)^{\frac{\alpha\gamma}{\alpha\gamma+1}} \frac{(1+\beta)^{\frac{\alpha\gamma}{\alpha\gamma+1}-\Gamma}}{(1+\beta^\gamma)^{\frac{\alpha\gamma}{\alpha\gamma+1}}} \\ &= \tilde{C}\left[\frac{1+\beta^\gamma}{(1+\beta)^\gamma}\right]^{\frac{1}{\alpha\gamma+1}} \end{aligned} \tag{A.4}$$

where $\tilde{C}$ is just a constant. We managed to write J as a function of β for the points on the stationary line. Now, we can conclude our exam by taking the derivative of the cost with respect to the ratio β:

$$\begin{aligned}\frac{\partial J(\beta)}{\partial \beta} &= \tilde{C}\left(\frac{1}{\alpha\gamma+1}\right)\left[\frac{1+\beta^{\gamma}}{(1+\beta)^{\gamma}}\right]^{\frac{1}{\alpha\gamma+1}-1}\frac{\gamma\beta^{\gamma-1}(1+\beta)^{\gamma}-(1+\beta^{\gamma})\gamma(1+\beta)^{\gamma-1}}{(1+\beta)^{2\gamma}} \\ &= g(\beta,\alpha,\gamma)\left[\beta^{\gamma-1}(1+\beta)^{\gamma}-(1+\beta^{\gamma})(1+\beta)^{\gamma-1}\right]\end{aligned} \tag{A.5}$$

since β is always positive it is easy to see that $g(\beta,\alpha,\gamma)$ is a positive non null function for every value of its arguments. Thus we can rewrite:

$$\begin{aligned}\frac{\partial J(\beta)}{\partial \beta}=0 \implies & \left[\beta^{\gamma-1}(1+\beta)^{\gamma}-(1+\beta^{\gamma})(1+\beta)^{\gamma-1}\right]=0 \\ \implies & \frac{\beta^{\gamma-1}-1}{1+\beta}=0\end{aligned} \tag{A.6}$$

the only stationary point is obtained for $\beta = 1$. This correspond to the symmetric loop configuration represented by the yellow point in Fig. A.3. Note that therefore, the only candidate minima for the model, are: the case for which $\beta = 1$, as just mentioned, and the case $\beta = 0, \infty$ that should be taken into account since they represent the extremal points of the stationary line on which we carried the final optimization. Hence, we have already proven that in the two resistor case the principle of local optimality is unnecessary and naturally come from the global optimization. Moreover, one can study the sign of A.5, that amounts on studying the sign of the numerator in A.6, and the final result, as expected, is that for $\gamma > 1$ the symmetrical loop is the absolute minimum, whereas for $0 < \gamma < 1$ we got the two solutions (C_1^*,0) and ($0, C_2^*$), that represent the only two trees that we can generate in this scenario. As last thing we were able to actually draw the cost function for this simple problem and it is displayed in Fig.A.4-A.5. Note that the bold line represent exactly the line of stationary points, marking a valley in the cost landscape. Even at eyesight we can verify the behaviour that we proved analytically. This approach can be further generalized in order to try to demonstrate the redundancy of the local optimality principle. However, as the size of the loops n_{loop} grow the computation become more and more cumbersome, in particular the number of constraints that we must consider in order to write the initial Lagrangian gets equal to $n_{loop} - 1$.

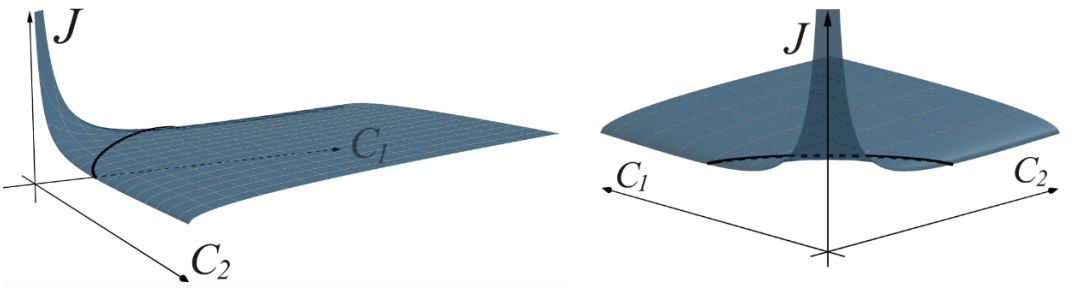

Figure A.4: 3D representation of $J(C_1, C_2)$ for $\gamma = 0.5$

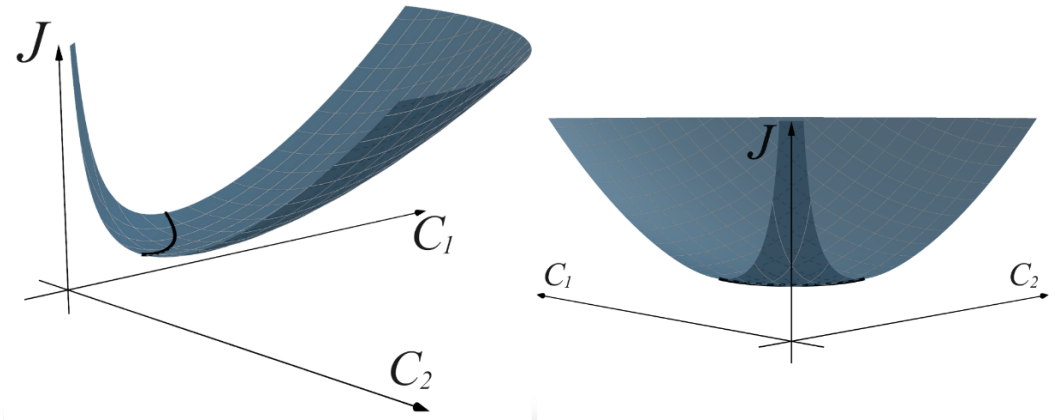

Figure A.5: 3D representation of $J(C_1, C_2)$ for $\gamma = 2$

Appendix B

Stability of stationary points

The reason why the stability of the stationary points (3.17) is delicate relies on the fact that the local perturbation of a conductance C_{ij}, in general, lead to a global perturbation of currents $\{Q_{ij}\}$. Thus even by perturbing only one conductance the currents have to adjust in a non trivial way that respect both the loads requirements and the Kirchoff's equation (3.9). At the end, the resulting flow $\bar{I}'$ will be the only possible solution for the new set of conductances $\bar{C}' = \{C_1, C_2, ..., C_i + \delta C, ..., C_{N_{edges}}\}$. As discussed previously, a straightforward analytical approach is problematic, thus let's try to follow another path.

In order to understand more clearly this issue, we can consider separately two different kind of conductances perturbations.

Definition 1. *Call A the set of edges in a network that are not part of any loop. Than all the perturbations $\delta\bar{C}$ of the type:*

$$\delta C_i = \begin{cases} 0, & i \in E \setminus A \\ \delta_i, & i \in A \end{cases} \tag{B.1}$$

are called tree-like fluctuations.

Lemma 3. *The stationary points (3.17) are stable to tree-like fluctuations.*

Proof. To prove it we can start from a generic loopy network and erase all the edges that are part of some loop. We should do that by imagining to exchange every loop with a single node, see Fig. B.1.

Note that, the fluxes exiting and entering the loop at each node, are always fixed. Furthermore, the flux entering a loop is unique (if not, it is because of another loop that we should erase first), and during the 'shrinking procedure' we have to modify its value to $Q'_{in} = Q_{in} - n_{loop} + 1$, where n_{loop} is the number of nodes in the loop. This will account for the nodes we are erasing, i.e. $(n_{loop} - 1)$ is the amount

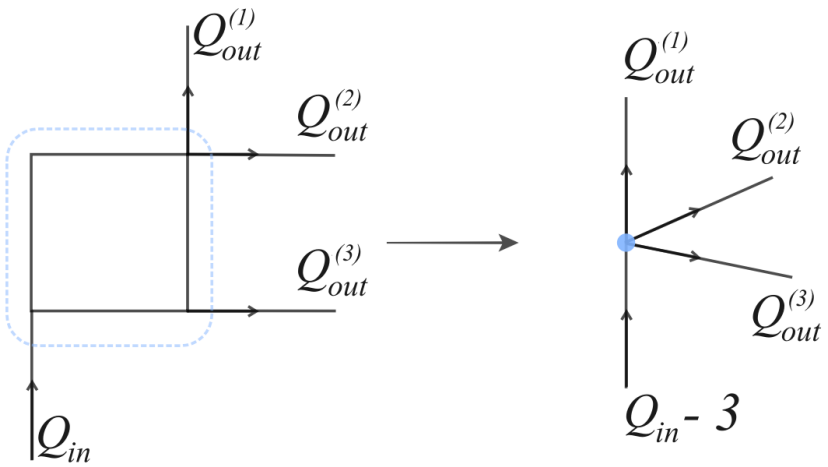

Figure B.1: Loop shrinking

of resources needed to feed the loop. Hence, the new network we have built is a tree that has exactly A as edges set. Now, for this tree it holds Lemma 2 meaning that a change of the conductances would not affect the currents. This imply that the stationary point (3.17) is stable on this network. But, since the currents don't change, the loop we have erased do not have a way to feel a perturbation of the conductances in A. Finally the latter imply that also in the original network, the stationary point (3.17) is stable to fluctuations of C_i with $i \in A$, i.e. tree-like fluctuations. □

Note that the perturbation of any edges for which $C_{ij} = 0$ would lead to a loop. That's why this kind of perturbation are not tree-like.

Definition 2. *Call B the set $E \setminus A$, where E is the set of all possible edges in our lattice. All the perturbations $\delta\bar{C}$ for which::*

$$\exists i \in B \mid \delta C_i \neq 0 \tag{B.2}$$

are called loop-like fluctuations.

Lemma 4. *Loop-like fluctuations make stationary points (3.17) unstable. For $\gamma < 1$ they can destruct loops whereas for $\gamma > 1$ they can generate them.*

To rigorously prove Lemma 4 would be an important step in order to demonstrate the redundancy of the local optimality principle. However, we were unable to provide such exact proof, in the following we develop only some instructive arguments.

We know that in this scenario the fluctuation of conductances lead also to a modification of the currents. An idea is then to start from a stationary point (3.17) and try to change the conductances in a way that the new state is still a stationary point of the same form for the new set of currents $\bar{Q}'$. The difficulty is that the currents can change only following some constraints, i.e. loads requirements and Kirchoff's equations (3.9). So let's try to describe a valid perturbation $\bar{Q}' = \bar{Q} + \delta\bar{Q}$ 'by hand'. We can generate it starting from a feasible flow distribution $\bar{Q}'$ and adding a constant flow δQ at each edge of any loop as shown in Fig. B.2.

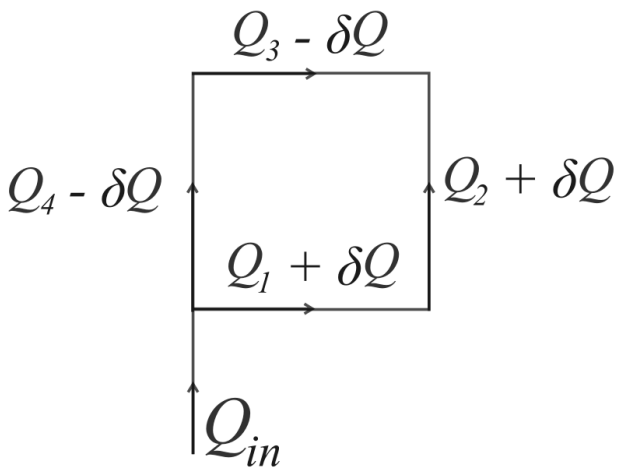

Figure B.2: Valid current fluctuation for a small loop

Note that if $-Q_1 \leq \delta Q \leq Q_4$ Kirchoff's equation can hold. We have thus built manually a valid perturbation of the currents (that nevertheless must have been generated by a conductances perturbation):

$$\delta Q_i = \begin{cases} 0 & , i \notin loop_k, \forall k \\ \delta_k & , i \in loop_k \end{cases} \tag{B.3}$$

note that we are implicitly defining a direction (clockwise or counterclockwise) for every loop and then the quantity δ_k is added for every edge (of the k'th loop) following the chosen direction. Furthermore observe that perturbation (B.3) can modify currents on all loops, also the ones we can build using some edges in witch $Q_i = 0$, i.e. this kind of fluctuation can actually form new loops.

At this point we can ask ourselves what should be the related stationary point for conductances. Using (3.15) we can write:

$$C_i' = C_i + \delta C_i = A_c (Q_i')^{\frac{\alpha+1}{\alpha\gamma+1}} = A_c (Q_i + \delta Q)^{\frac{\alpha+1}{\alpha\gamma+1}} \tag{B.4}$$

but now from B.4, considering that δQ is a small perturbation (i.e. $\frac{\delta Q}{Q} \ll 1$), we can compute what should be the initial perturbation on the conductances in order to produce a currents variation δQ :

$$\delta C_i \approx A_c \frac{\alpha+1}{\alpha\gamma+1} Q_i^{\frac{\alpha+1}{\alpha\gamma+1}-1} \delta Q \tag{B.5}$$

$$= c\, Q_i^{\frac{\alpha(1-\gamma)}{\alpha\gamma+1}} \delta Q \qquad , c > 0 \tag{B.6}$$

thus, the flows fluctuation (B.3) can be produced by the conductances fluctuation:

$$\delta C_i = \begin{cases} 0 & , i \notin loop_k, \forall k \\ c\, Q_i^{\frac{\alpha(1-\gamma)}{\alpha\gamma+1}} \delta_k & , i \in loop_k \end{cases} \tag{B.7}$$

we have reached a good result but we still lack something. In fact we still haven't proven that the perturbation (B.7) lead to (B.3) following the constraints (3.9). In fact, we should reason in the opposite sense. Let's start with a loop-like fluctuation as (B.7). Now, as we proven in Lemma 1, there will be an unique distribution of pressure gradients fulfilling the Khirchoff equations. So a new pressure gradient $\Delta p_i' = \Delta p_i + \delta(\Delta p_i)$ is defined at all edges of the perturbed loop. Then the unique solution for the flows is enforced by the dynamical flow equation:

$$\begin{aligned} Q_i' &= C_i' \Delta p_i' \\ Q_i + \delta Q_i &= (C_i + \delta C_i)(\Delta p_i + \delta(\Delta p_i)) \\ \implies \delta Q_i &\approx C_i \delta(\Delta p_i) + \delta C_i \Delta p_i \\ \implies \delta Q_i &\approx B C_i \delta(\Delta p_i) \end{aligned} \tag{B.8}$$

where we used for δC_i and Δp_i the expressions valid at the stationary point and B is a constant. Furthermore, we can observe that in order to fulfill even the loads requirements (i.e. the continuity equation), the only valid perturbation of the currents is a constant perturbation δQ with the same sign in a given direction of the loop. So in the end we can consider $\delta Q_i = \delta Q$. Taking a sum on the loop in (B.8) we can show that we are able to generate exactly a flows perturbation of type (B.3) , where δQ is:

$$\delta Q \propto \frac{1}{n_{loop}} \sum_{i \in loop} C_i \delta(\Delta p_i) \tag{B.9}$$

the latter can be seen as a self-consistent equation for δQ if we consider that the fluctuations in the pressure gradients depends on δQ. Unfortunately we weren't able to prove that it exists a δQ satisfying such self-consistent equation. Although, the satisfiability of (B.9) would imply that we are able to manually describe a fluctuation of the conductances (B.7) for which flows change in a valid way (B.3), following all the constraints (3.9). Most importantly both the starting and the ending states $(\bar{C}, \bar{I})$ and $(\bar{C}+\delta\bar{C}, \bar{I}+\delta\bar{C})$ are stationary points (3.17) and therefore we can draw a continuous stationary line in the Ω space as displayed in Fig. B.3.

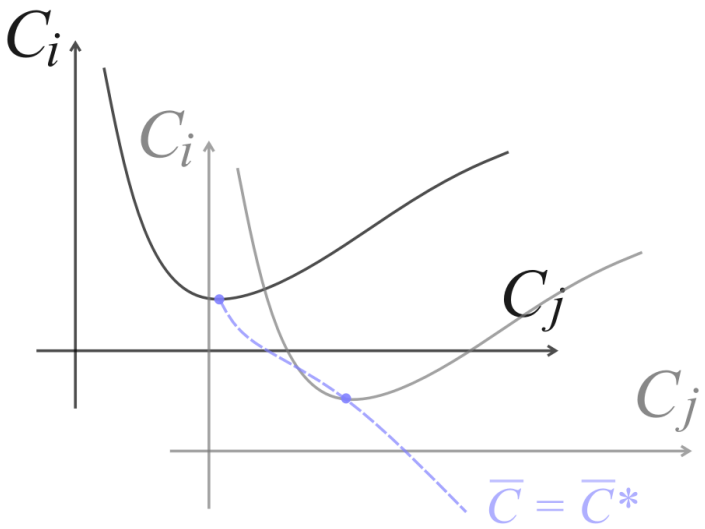

Figure B.3: Stationary line in Ω space

If we postulate the existence of such line, there are two ways to actually prove Lemma 4. The first consist in observing that a chain of fluctuations, as the ones we just described, allows a flow in the Ω space along the stationary line. On this trajectory we can rewrite the total cost function using (3.15), we obtain:

$$J \propto \sum_{ij} Q_{ij}^{\Gamma} \qquad \textit{with} \quad \Gamma > 1 \Leftrightarrow \gamma > 1 \quad \textit{and} \quad 0 < \Gamma < 1 \Leftrightarrow 0 < \gamma < 1 \tag{B.10}$$

but this model has been exactly studied by Banavar [39], who has proven that for $\Gamma > 1$ the only minimum of the cost function is the completely loopy network, whereas for $0 < \Gamma < 1$ the trees are the only minima. This prove that for $\gamma > 1$ loop-like fluctuations will allow for every loop to generate, while instead for $0 < \Gamma < 1$ the same fluctuations can destroy any loop and thus the only stable stationary points are tree-like nets.

Proof. - Version 2 - On the other hand, we can also proceed in another direction without using Banavar results. We included this reasoning because we find it illustrative and because it represent an alternative original version of the central Banavar's proof. We can use (B.3) and (B.7) to approximate the change in the cost function (B.10):

$$\begin{aligned} J' &\propto \sum_{ij} (Q_{ij} + \delta Q_{ij})^{\Gamma} \\ &\approx J + \sum_{ij} [\Gamma Q_{ij}^{\Gamma-1}] \ \delta Q_{ij} \\ &= J + \delta J \end{aligned} \tag{B.11}$$

now, we can look at what happens at δJ, for different values of Γ, when we try to generate or destroy a loop. Let's for instance consider the case $0 < \Gamma < 1$. We start from a stationary loopy network and try to destroy a loop. To do so one of the edges of the loop, let's call it C_{j_0} should go to zero. Can a fluctuations chain of the type we just described be able to destroy an edge? The answer is yes. We can show it by perturbing the loop in which there is C_{j_0} and looking at the behaviour δJ, in fact from eq (B.12) we can write:

$$\begin{aligned} \delta J &\approx \sum_{i \in loop} [\Gamma Q_i^{\Gamma-1}] \ \delta Q_i \\ &= [\Gamma Q_{j_0}^{\Gamma-1}] \ \delta Q_{j_0} + \sum_{i \in loop \setminus j_0} [\Gamma Q_i^{\Gamma-1}] \ \delta Q_i \end{aligned} \tag{B.12}$$

remember that if we want to destroy a loop, Q_{j_0} should go to zero, implying $Q_{j_0} \ll Q_i$. Thus we have:

$$\lim_{Q_{j_0} \to 0} Q_{j_0}^{\Gamma-1} \delta Q = \begin{cases} \ll Q_i^{\Gamma-1} \delta Q & \Gamma > 1 \\ \gg Q_i^{\Gamma-1} \delta Q & 0 < \Gamma < 1 \end{cases} \tag{B.13}$$

the latter is a truly insightful relation that tell us what is the relative weight of terms in (B.12) when we try to lead one conductance to zero. Now if we start from the case $0 < \Gamma < 1$ ($0 < \gamma < 1$), we see that the leading term is the one related to Q_{j_0}, implying that in this case we can further simplify (B.12) as:

$$\delta J \approx [\Gamma Q_{j_0}^{\Gamma-1}] \ \delta Q_{j_0} \tag{B.14}$$

but, since $Q_{j_0} > 0$ and δQ should be negative if we want to destroy the loop, δJ is negative too. Thus, indeed in this regime loop-like fluctuations can destroy loops. For the same reason a loop can't be originated from a tree in this regime ($\delta Q > 0 \implies \delta J > 0$).

On the other hand, the situation is slightly more complex for $\Gamma > 1$ ($\gamma > 1$). In this case (B.12) reads:

$$\delta J \approx \sum_{i \in loop \setminus j_0} [\Gamma Q_i^{\Gamma-1}] \ \delta Q_i \tag{B.15}$$

let's say that now we want to start from a tree and try to create a loop 'switching on' a new edge. In this case the sign of δJ is more complicated to capture because each term in (B.15) can either be positive or negative. In fact δQ_i is equal in modulus for each edge but can represent either a growth or a decrease for different edges in the loop. The interesting thing is that even if $\delta J > 0$, for sure, if we consider a similar fluctuation in which we invert the sign of the extra perturbation current δQ we are sending in the loop, now $\delta J < 0$. Meaning that if we want to switch on a current on the *(ij)* edge we can always do it either in the $i \to j$ direction or in the $j \to i$ one. Note that this mean that there exist some unstable loops too, but is easy to show that any unstable loop can evolve toward a stable one. This proves that for $\gamma > 1$ loop-like fluctuations can generate new loops and thus the only stable stationary point is the completely loopy network. □

Acknowledgements

I extend my heartfelt gratitude to several people who supported me along this academic journey. First and foremost, my deepest thanks go to my family for their unwavering support throughout these years. Their encouragement and understanding have been to me of fundamental importance . I am thankful to my supervisor, Luca Ridolfi, for his profound care and guidance during our collaborative work. His expertise, dedication, and the captivating subject of research he provided have enriched my academic experience and contributed significantly to the development of this thesis. Special thanks are due to Amilcare Porporato for hosting me at Princeton, providing valuable insights and deeply contributing to my research experience. Finally, I would also like to acknowledge the support and collaboration shared by my colleague, PhD Shashank Anand, which added a valuable dimension to the overall research process.

Bibliography

[1] Thomas Young. «XIII. Hydraulic investigations, subservient to an intended Croonian Lecture on the motion of the blood». In: *Philosophical Transactions of the Royal Society of London* 98 (Jan. 1997). Publisher: Royal Society, pp. 164–186. DOI: 10.1098/rstl.1808.0014. URL: https://royalsocietypublishing.org/doi/10.1098/rstl.1808.0014 (visited on 11/03/2023) (cit. on p. 4).

[2] W. R. Hess. «Über die periphere Regulierung der Blutzirkulation». de. In: *Pflüger's Archiv für die gesamte Physiologie des Menschen und der Tiere* 168.9 (Aug. 1917), pp. 439–490. ISSN: 1432-2013. DOI: 10.1007/BF01681580. URL: https://doi.org/10.1007/BF01681580 (visited on 11/03/2023) (cit. on p. 4).

[3] Cecil D. Murray. *The Physiological Principle of Minimum Work*. en. 1926. DOI: 10.1073/pnas.12.3.207. URL: https://www.pnas.org/doi/10.1073/pnas.12.3.207 (visited on 10/14/2023) (cit. on pp. 4, 26, 31, 35).

[4] Enrico Sciubba. «A Critical Reassessment of the Hess–Murray Law». en. In: *Entropy* 18.8 (Aug. 2016). Number: 8 Publisher: Multidisciplinary Digital Publishing Institute, p. 283. ISSN: 1099-4300. DOI: 10.3390/e18080283. URL: https://www.mdpi.com/1099-4300/18/8/283 (visited on 10/14/2023) (cit. on p. 5).

[5] H B M Uylings. «Optimization of diameters and bifurcation angles in lung and vascular tree structures». en. In: (1977) (cit. on pp. 5, 35).

[6] Geoffrey B. West, James H. Brown, and Brian J. Enquist. «A General Model for the Origin of Allometric Scaling Laws in Biology». In: *Science* 276.5309 (Apr. 1997). Publisher: American Association for the Advancement of Science, pp. 122–126. DOI: 10.1126/science.276.5309.122. URL: https://www.science.org/doi/10.1126/science.276.5309.122 (visited on 11/09/2023) (cit. on pp. 5, 36).

[7] Antonio F. Miguel. «A study of entropy generation in tree-shaped flow structures». en. In: *International Journal of Heat and Mass Transfer* 92 (Jan. 2016), pp. 349–359. ISSN: 00179310. DOI: 10.1016/j.ijheatmasstransfer.2015.08.067. URL: https://linkinghub.elsevier.com/retrieve/pii/S0017931015301976 (visited on 11/03/2023) (cit. on p. 5).

[8] Dai Akita, Itsuki Kunita, Mark D Fricker, Shigeru Kuroda, Katsuhiko Sato, and Toshiyuki Nakagaki. «Experimental models for Murray's law». en. In: *Journal of Physics D: Applied Physics* 50.2 (Jan. 2017), p. 024001. ISSN: 0022-3727, 1361-6463. DOI: 10.1088/1361-6463/50/2/024001. URL: https://iopscience.iop.org/article/10.1088/1361-6463/50/2/024001 (visited on 10/14/2023) (cit. on pp. 5, 12, 13).

[9] Yunlong Huo and Ghassan S. Kassab. «Intraspecific scaling laws of vascular trees». en. In: *Journal of The Royal Society Interface* 9.66 (Jan. 2012), pp. 190–200. ISSN: 1742-5689, 1742-5662. DOI: 10.1098/rsif.2011.0270. URL: https://royalsocietypublishing.org/doi/10.1098/rsif.2011.0270 (visited on 11/09/2023) (cit. on p. 5).

[10] Wang Zhi, Zhao Ming, and Yu Qi-Xing. «Modeling of Branching Structures of Plants». en. In: *Journal of Theoretical Biology* 209.4 (Apr. 2001), pp. 383–394. ISSN: 00225193. DOI: 10.1006/jtbi.2001.2252. URL: https://linkinghub.elsevier.com/retrieve/pii/S0022519301922520 (visited on 11/11/2023) (cit. on p. 5).

[11] Mitchell G. Newberry, Daniel B. Ennis, and Van M. Savage. «Testing Foundations of Biological Scaling Theory Using Automated Measurements of Vascular Networks». en. In: *PLOS Computational Biology* 11.8 (2015). Publisher: Public Library of Science, e1004455. ISSN: 1553-7358. DOI: 10.1371/journal.pcbi.1004455. URL: https://journals.plos.org/ploscompbiol/article?id=10.1371/journal.pcbi.1004455 (visited on 10/16/2023) (cit. on p. 5).

[12] Katherine A. McCulloh, John S. Sperry, and Frederick R. Adler. «Water transport in plants obeys Murray's law». en. In: *Nature* 421.6926 (Feb. 2003), pp. 939–942. ISSN: 0028-0836, 1476-4687. DOI: 10.1038/nature01444. URL: https://www.nature.com/articles/nature01444 (visited on 11/11/2023) (cit. on p. 5).

[13] T F Sherman. «On connecting large vessels to small. The meaning of Murray's law.» en. In: *The Journal of general physiology* 78.4 (Oct. 1981), pp. 431–453. ISSN: 0022-1295, 1540-7748. DOI: 10.1085/jgp.78.4.431. URL: https://rupress.org/jgp/article/78/4/431/27121/On-connecting-large-vessels-to-small-The-meaning (visited on 11/03/2023) (cit. on p. 6).

[14] Andrea Rinaldo, Ignacio Rodriguez-Iturbe, Riccardo Rigon, Rafael L. Bras, Ede Ijjasz-Vasquez, and Alessandro Marani. «Minimum energy and fractal structures of drainage networks». en. In: *Water Resources Research* 28.9 (1992), pp. 2183–2195. ISSN: 1944-7973. DOI: 10.1029/92WR00801. URL: https://onlinelibrary.wiley.com/doi/abs/10.1029/92WR00801 (visited on 10/14/2023) (cit. on p. 7).

[15] Ignacio Rodríguez-Iturbe, Andrea Rinaldo, Riccardo Rigon, Rafael L. Bras, Alessandro Marani, and Ede Ijjász-Vásquez. «Energy dissipation, runoff production, and the three-dimensional structure of river basins». en. In: *Water Resources Research* 28.4 (1992), pp. 1095–1103. ISSN: 1944-7973. DOI: 10.1029/91WR03034. URL: https://onlinelibrary.wiley.com/doi/abs/10.1029/91WR03034 (visited on 10/14/2023) (cit. on p. 7).

[16] Andrea Rinaldo, Jayanth R. Banavar, and Amos Maritan. «Trees, networks, and hydrology». en. In: *Water Resources Research* 42.6 (2006). _eprint: https://onlinelibrary.wiley.com/doi/pdf/10.1029/2005WR004108. ISSN: 1944-7973. DOI: 10.1029/2005WR004108. URL: https://onlinelibrary.wiley.com/doi/abs/10.1029/2005WR004108 (visited on 10/14/2023) (cit. on p. 7).

[17] Ignacio Rodríguez-Iturbe and Andrea Rinaldo. *Fractal River Basins: Chance and Self-Organization*. en. Google-Books-ID: _xjhtl7zeB8C. Cambridge University Press, 1997. ISBN: 978-0-521-00405-3 (cit. on pp. 7, 52).

[18] Jayanth R. Banavar, Francesca Colaiori, Alessandro Flammini, Amos Maritan, and Andrea Rinaldo. «Topology of the Fittest Transportation Network». en. In: *Physical Review Letters* 84.20 (May 2000), pp. 4745–4748. ISSN: 0031-9007, 1079-7114. DOI: 10.1103/PhysRevLett.84.4745. URL: https://link.aps.org/doi/10.1103/PhysRevLett.84.4745 (visited on 10/14/2023) (cit. on pp. 8, 32).

[19] Steffen Bohn and Marcelo O. Magnasco. «Structure, Scaling, and Phase Transition in the Optimal Transport Network». en. In: *Physical Review Letters* 98.8 (Feb. 2007), p. 088702. ISSN: 0031-9007, 1079-7114. DOI: 10.1103/PhysRevLett.98.088702. URL: https://link.aps.org/doi/10.1103/PhysRevLett.98.088702 (visited on 10/14/2023) (cit. on pp. 8, 9, 35).

[20] Francis Corson. «Fluctuations and Redundancy in Optimal Transport Networks». en. In: *Physical Review Letters* 104.4 (Jan. 2010), p. 048703. ISSN: 0031-9007, 1079-7114. DOI: 10.1103/PhysRevLett.104.048703. URL: https://link.aps.org/doi/10.1103/PhysRevLett.104.048703 (visited on 10/16/2023) (cit. on pp. 10, 35).

[21] Eleni Katifori, Gergely J. Szöllősi, and Marcelo O. Magnasco. «Damage and Fluctuations Induce Loops in Optimal Transport Networks». en. In: *Physical Review Letters* 104.4 (Jan. 2010), p. 048704. ISSN: 0031-9007, 1079-7114. DOI: 10.1103/PhysRevLett.104.048704. URL: https://link.aps.org/doi/10.1103/PhysRevLett.104.048704 (visited on 10/30/2023) (cit. on pp. 10, 11, 35).

[22] Alessandro Lonardi, Enrico Facca, Mario Putti, and Caterina De Bacco. «Infrastructure adaptation and emergence of loops in network routing with time-dependent loads». en. In: *Physical Review E* 107.2 (Feb. 2023), p. 024302. ISSN: 2470-0045, 2470-0053. DOI: 10.1103/PhysRevE.107.024302. URL: https://link.aps.org/doi/10.1103/PhysRevE.107.024302 (visited on 10/16/2023) (cit. on pp. 11, 35).

[23] Enrico Facca, Franco Cardin, and Mario Putti. «Branching structures emerging from a continuous optimal transport model». en. In: *Journal of Computational Physics* 447 (Dec. 2021), p. 110700. ISSN: 00219991. DOI: 10.1016/j.jcp.2021.110700. URL: https://linkinghub.elsevier.com/retrieve/pii/S0021999121005957 (visited on 10/16/2023) (cit. on pp. 11, 36).

[24] Yuankai Lu and Dan Hu. «Optimisation of Biological Transport Networks». en. In: *East Asian Journal on Applied Mathematics* 12.1 (June 2022), pp. 72–95. ISSN: 2079-7362, 2079-7370. DOI: 10.4208/eajam.180521.130721. URL: http://global-sci.org/intro/article_detail/eajam/19921.html (visited on 10/14/2023) (cit. on p. 12).

[25] Dan Hu and David Cai. «Adaptation and Optimization of Biological Transport Networks». en. In: *Physical Review Letters* 111.13 (Sept. 2013), p. 138701. ISSN: 0031-9007, 1079-7114. DOI: 10.1103/PhysRevLett.111.138701. URL: https://link.aps.org/doi/10.1103/PhysRevLett.111.138701 (visited on 10/14/2023) (cit. on pp. 12, 13, 35).

[26] Rodrigo Almeida and Rui Dilão. «Adaptive Hagen–Poiseuille flows on graphs». In: *Physica D: Nonlinear Phenomena* 436 (Aug. 2022), p. 133322. ISSN: 0167-2789. DOI: 10.1016/j.physd.2022.133322. URL: https://www.sciencedirect.com/science/article/pii/S0167278922001014 (visited on 10/14/2023) (cit. on pp. 12, 36).

[27] Dan Hu and David Cai. «An optimization principle for initiation and adaptation of biological transport networks». en. In: *Communications in Mathematical Sciences* 17.5 (2019), pp. 1427–1436. ISSN: 15396746, 19450796. DOI: 10.4310/CMS.2019.v17.n5.a12. URL: https://www.intlpress.com/site/pub/pages/journals/items/cms/content/vols/0017/0005/a012/ (visited on 10/14/2023) (cit. on p. 12).

[28] Enrico Facca, Franco Cardin, and Mario Putti. «Towards a Stationary Monge–Kantorovich Dynamics: The Physarum Polycephalum Experience». In: *SIAM Journal on Applied Mathematics* 78.2 (Jan. 2018). Publisher: Society for Industrial and Applied Mathematics, pp. 651–676. ISSN: 0036-1399. DOI: 10.1137/16M1098383. URL: https://epubs.siam.org/doi/10.1137/16M1098383 (visited on 10/16/2023) (cit. on p. 12).

[29] Henrik Ronellenfitsch and Eleni Katifori. «Phenotypes of Vascular Flow Networks». en. In: *Physical Review Letters* 123.24 (Dec. 2019), p. 248101. ISSN: 0031-9007, 1079-7114. DOI: 10.1103/PhysRevLett.123.248101. URL: https://link.aps.org/doi/10.1103/PhysRevLett.123.248101 (visited on 10/14/2023) (cit. on pp. 12, 35).

[30] Atsushi Tero, Seiji Takagi, Tetsu Saigusa, Kentaro Ito, Dan P. Bebber, Mark D. Fricker, Kenji Yumiki, Ryo Kobayashi, and Toshiyuki Nakagaki. «Rules for Biologically Inspired Adaptive Network Design». In: *Science* 327.5964 (Jan. 2010). Publisher: American Association for the Advancement of Science, pp. 439–442. DOI: 10.1126/science.1177894. URL: https://www.science.org/doi/10.1126/science.1177894 (visited on 10/15/2023) (cit. on p. 12).

[31] Atsushi Tero, Ryo Kobayashi, and Toshiyuki Nakagaki. «A mathematical model for adaptive transport network in path finding by true slime mold». In: *Journal of Theoretical Biology* 244.4 (Feb. 2007), pp. 553–564. ISSN: 0022-5193. DOI: 10.1016/j.jtbi.2006.07.015. URL: https://www.sciencedirect.com/science/article/pii/S002251930600289X (visited on 10/16/2023) (cit. on p. 12).

[32] Vincenzo Bonifaci, Kurt Mehlhorn, and Girish Varma. «Physarum can compute shortest paths». In: *Journal of Theoretical Biology* 309 (Sept. 2012), pp. 121–133. ISSN: 0022-5193. DOI: 10.1016/j.jtbi.2012.06.017. URL: https://www.sciencedirect.com/science/article/pii/S0022519312003049 (visited on 11/08/2023) (cit. on p. 12).

[33] Timothy W. Secomb, Jonathan P. Alberding, Richard Hsu, Mark W. Dewhirst, and Axel R. Pries. «Angiogenesis: An Adaptive Dynamic Biological Patterning Problem». en. In: *PLOS Computational Biology* 9.3 (Mar. 2013). Publisher: Public Library of Science, e1002983. ISSN: 1553-7358. DOI: 10.1371/journal.pcbi.1002983. URL: https://journals.plos.org/ploscompbiol/article?id=10.1371/journal.pcbi.1002983 (visited on 11/07/2023) (cit. on p. 13).

[34] Qi Chen, Luan Jiang, Chun Li, Dan Hu, Ji-wen Bu, David Cai, and Jiu-lin Du. «Haemodynamics-Driven Developmental Pruning of Brain Vasculature in Zebrafish». en. In: *PLOS Biology* 10.8 (2012). Publisher: Public Library of Science, e1001374. ISSN: 1545-7885. DOI: 10.1371/journal.pbio.1001374.

URL: https://journals.plos.org/plosbiology/article?id=10.1371/journal.pbio.1001374 (visited on 11/07/2023) (cit. on p. 13).

[35] Lewis F. Moody. «Friction factors for pipe flow». In: *Transactions of the American Society of Mechanical Engineers* 66.8 (1944). Publisher: American Society of Mechanical Engineers, pp. 671–678. URL: https://asmedigitalcollection.asme.org/fluidsengineering/article-abstract/66/8/671/1153865 (visited on 11/13/2023) (cit. on p. 20).

[36] R. J. Duffin. «Nonlinear networks. IIa». In: *Bulletin of the American Mathematical Society* 53.10 (Oct. 1947). Publisher: American Mathematical Society, pp. 963–971. ISSN: 0002-9904, 1936-881X. URL: https://projecteuclid.org/journals/bulletin-of-the-american-mathematical-society/volume-53/issue-10/Nonlinear-networks-IIa/bams/1183511146.full (visited on 11/03/2023) (cit. on p. 23).

[37] Marc Durand. «Architecture of optimal transport networks». en. In: *Physical Review E* 73.1 (Jan. 2006), p. 016116. ISSN: 1539-3755, 1550-2376. DOI: 10.1103/PhysRevE.73.016116. URL: https://link.aps.org/doi/10.1103/PhysRevE.73.016116 (visited on 10/16/2023) (cit. on p. 26).

[38] COLIN CHERRY. «Non-linear circuit theory by the methods of classical dynamics». In: *Recent Developments in Network Theory*. Elsevier, 1963, pp. 211–219. URL: https://www.sciencedirect.com/science/article/pii/B9781483198538500172 (visited on 11/14/2023) (cit. on p. 26).

[39] Andrea Rinaldo, Riccardo Rigon, Jayanth R. Banavar, Amos Maritan, and Ignacio Rodriguez-Iturbe. «Evolution and selection of river networks: Statics, dynamics, and complexity». en. In: *Proceedings of the National Academy of Sciences* 111.7 (Feb. 2014), pp. 2417–2424. ISSN: 0027-8424, 1091-6490. DOI: 10.1073/pnas.1322700111. URL: https://pnas.org/doi/full/10.1073/pnas.1322700111 (visited on 10/23/2023) (cit. on pp. 32, 52, 74).

[40] Marc Durand. «Structure of Optimal Transport Networks Subject to a Global Constraint». en. In: *Physical Review Letters* 98.8 (Feb. 2007), p. 088701. ISSN: 0031-9007, 1079-7114. DOI: 10.1103/PhysRevLett.98.088701. URL: https://link.aps.org/doi/10.1103/PhysRevLett.98.088701 (visited on 10/16/2023) (cit. on p. 36).

[41] S. Kirkpatrick, C. D. Gelatt, and M. P. Vecchi. «Optimization by Simulated Annealing». In: *Science* 220.4598 (May 1983). Publisher: American Association for the Advancement of Science, pp. 671–680. DOI: 10.1126/science.220.4598.671. URL: https://www.science.org/doi/10.1126/science.220.4598.671 (visited on 11/08/2023) (cit. on p. 47).

[42] Walid Ben-Ameur. «Computing the Initial Temperature of Simulated Annealing». en. In: *Computational Optimization and Applications* 29.3 (Dec. 2004), pp. 369–385. ISSN: 0926-6003. DOI: 10.1023/B:COAP.0000044187.23143.bd. URL: http://link.springer.com/10.1023/B:COAP.0000044187.23143.bd (visited on 10/17/2023) (cit. on p. 47).

[43] Mir M. Atiqullah. *Computational science and its applications - ICCSA 2004. 3*. en. Lecture notes in computer science 3045. Berlin Heidelberg: Springer, 2004. ISBN: 978-3-540-22057-2 (cit. on pp. 47, 48).

[44] Brent M. Troutman and Michael R. Karlinger. «Gibbs' Distribution on drainage networks». en. In: *Water Resources Research* 28.2 (1992). _eprint: https://onlinelibrary.wiley.com/doi/pdf/10.1029/91WR02648, pp. 563–577. ISSN: 1944-7973. DOI: 10.1029/91WR02648. URL: https://onlinelibrary.wiley.com/doi/abs/10.1029/91WR02648 (visited on 11/15/2023) (cit. on p. 50).

[45] Andrea Rinaldo, Amos Maritan, Francesca Colaiori, Alessandro Flammini, Riccardo Rigon, Ignacio Rodriguez-Iturbe, and Jayanth R. Banavar. «Thermodynamics of Fractal Networks». en. In: *Physical Review Letters* 76.18 (Apr. 1996), pp. 3364–3367. ISSN: 0031-9007, 1079-7114. DOI: 10.1103/PhysRevLett.76.3364. URL: https://link.aps.org/doi/10.1103/PhysRevLett.76.3364 (visited on 10/14/2023) (cit. on pp. 50, 52).

[46] S. Bonetti, A. D. Bragg, and A. Porporato. «On the theory of drainage area for regular and non-regular points». In: *Proceedings of the Royal Society A: Mathematical, Physical and Engineering Sciences* 474.2211 (Mar. 2018). Publisher: Royal Society, p. 20170693. DOI: 10.1098/rspa.2017.0693. URL: https://royalsocietypublishing.org/doi/10.1098/rspa.2017.0693 (visited on 10/16/2023) (cit. on p. 51).

[47] I. Rodríguez-Iturbe, E. J. Ijjász-Vásquez, R. L. Bras, and D. G. Tarboton. «Power law distributions of discharge mass and energy in river basins». en. In: *Water Resources Research* 28.4 (1992), pp. 1089–1093. ISSN: 1944-7973. DOI: 10.1029/91WR03033. URL: https://onlinelibrary.wiley.com/doi/abs/10.1029/91WR03033 (visited on 10/14/2023) (cit. on p. 51).

[48] Milad Hooshyar, Shashank Anand, and Amilcare Porporato. «Variational analysis of landscape elevation and drainage networks». en. In: *Proceedings of the Royal Society A: Mathematical, Physical and Engineering Sciences* 476.2239 (July 2020), p. 20190775. ISSN: 1364-5021, 1471-2946. DOI: 10.1098/rspa.2019.0775. URL: https://royalsocietypublishing.org/doi/10.1098/rspa.2019.0775 (visited on 10/14/2023) (cit. on p. 51).

[49] ROBERT E HORTON. «EROSIONAL DEVELOPMENT OF STREAMS AND THEIR DRAINAGE BASINS; HYDROPHYSICAL APPROACH TO QUANTITATIVE MORPHOLOGY». In: *GSA Bulletin* 56.3 (Mar. 1945), pp. 275–370. ISSN: 0016-7606. DOI: 10.1130/0016-7606(1945)56[275:EDOSAT]2.0.CO;2. URL: https://doi.org/10.1130/0016-7606(1945)56[275:EDOSAT]2.0.CO;2 (visited on 11/17/2023) (cit. on p. 52).

[50] J. T. Hack. «Studies of longitudinal stream profiles in Virginia and Maryland». en. In: *Professional Paper* (1957). Number: 294-B. ISSN: 2330-7102. DOI: 10.3133/pp294B. URL: https://pubs.usgs.gov/publication/pp294B (visited on 11/17/2023) (cit. on p. 52).

[51] Per Bak. *How Nature Works: the science of self-organized criticality*. en. Google-Books-ID: x8nSBwAAQBAJ. Springer Science & Business Media, Nov. 2013. ISBN: 978-1-4757-5426-1 (cit. on p. 52).

[52] F. Colaiori, A. Flammini, A. Maritan, and J. R. Banavar. «An Analytical and Numerical Study of Optimal Channel Networks». In: *Physical Review E* 55.2 (Feb. 1997). arXiv:cond-mat/9610004, pp. 1298–1310. ISSN: 1063-651X, 1095-3787. DOI: 10.1103/PhysRevE.55.1298. URL: http://arxiv.org/abs/cond-mat/9610004 (visited on 11/09/2023) (cit. on pp. 52, 53).

[53] Amos Maritan, Andrea Rinaldo, Riccardo Rigon, Achille Giacometti, and Ignacio Rodríguez-Iturbe. «Scaling laws for river networks». en. In: *Physical Review E* 53.2 (Feb. 1996), pp. 1510–1515. ISSN: 1063-651X, 1095-3787. DOI: 10.1103/PhysRevE.53.1510. URL: https://link.aps.org/doi/10.1103/PhysRevE.53.1510 (visited on 11/10/2023) (cit. on p. 52).

[54] Amos Maritan, Francesca Colaiori, Alessandro Flammini, Marek Cieplak, and Jayanth R. Banavar. «Universality Classes of Optimal Channel Networks». en. In: *Science* 272.5264 (May 1996), pp. 984–986. ISSN: 0036-8075, 1095-9203. DOI: 10.1126/science.272.5264.984. URL: https://www.science.org/doi/10.1126/science.272.5264.984 (visited on 10/14/2023) (cit. on p. 53).

[55] A. Flammini and F. Colaiori. «Exact analysis of the Peano basin». en. In: *Journal of Physics A: Mathematical and General* 29.21 (Nov. 1996), p. 6701. ISSN: 0305-4470. DOI: 10.1088/0305-4470/29/21/006. URL: https://dx.doi.org/10.1088/0305-4470/29/21/006 (visited on 11/25/2023) (cit. on p. 55).